

Springback

R.H. Wagoner, J.F. Wang, and M. Li, The Ohio State University

This article is intended as an introduction to the concepts of springback simulation as well as recommendations for its practice in a metal forming setting. Most of the developments focus on thin beams or sheets, where springback is most pronounced. The underlying mechanics of large-strain, elastic-plastic deformation are treated in a simplified, intuitive way, with numerous references provided for those wishing to delve into the theoretical underpinnings in more detail. Simple bending is first considered, along with a discussion of approximations, then bending with tension and finally, more complex numerical treatments. Compensation of die design to account for springback is also presented briefly.

This treatment is intended for practitioners with widely differing backgrounds and needs. The early treatments are suited to a limited class of problems but are best suited for understanding the direction of the effects of various material properties and process parameters. The roles and effects of various simplifying assumptions are also treated naturally with these closed-form solutions. The later treatments are intended to augment the practice of applied sheet forming

analysis (almost always finite element based) to include postforming springback analysis. As is shown, the choices of numerical parameters can be quite different for springback, so these aspects are emphasized.

As used throughout this article, *springback* refers to the elastically driven change of shape that occurs after deforming a body and then releasing it. The concept is understood by anyone who has manually bent a metal wire or strip. For a sufficiently small bend radius, some part of the bending remains after unloading and some part is recovered during unloading (or has sprung back). For bend radii larger than some critical value, the initial shape of the body is recovered. The recovered portion of the deformation is referred to as springback. As such, the definition inherently refers to a difference in geometry between the loaded state and the unloaded state.

The word *springback* as a single, unhyphenated word appears in virtually no standard dictionaries but has been in technical use since at least the early 1940s. A search of the internet in April 2005 found more than 26,800 occurrences of the word, and a contemporaneous search of the ISI Web of Science (Thomson

Scientific) of published technical papers located 334 such references appearing since 1980. These numbers represent increases of 460 and 27%, respectively, over similar searches performed 20 months earlier, in April 2003. Two inferences may be drawn: the technical meaning of springback is well established, although formal definitions appearing in dictionaries lag, and interest in springback is growing rapidly.

The definition of springback can be broad, applying to the action of springs, for example, but the principal technical intent of the word and interest in the phenomenon refers to the undesirable shape change that occurs after forming a part. The change is undesirable because it creates a difference of part shape from the tool shapes that were used to carry out the forming operation. If this difference is not predicted accurately and compensated for in the design of the tools, the part may not meet specifications.

Consideration of springback is of prime interest for bodies that have high aspect ratios; that is, at least one dimension is much larger than, or smaller than, the other dimensions. Examples include slender beams and thin sheets (Fig. 1, 2). For these cases, the overall geometric

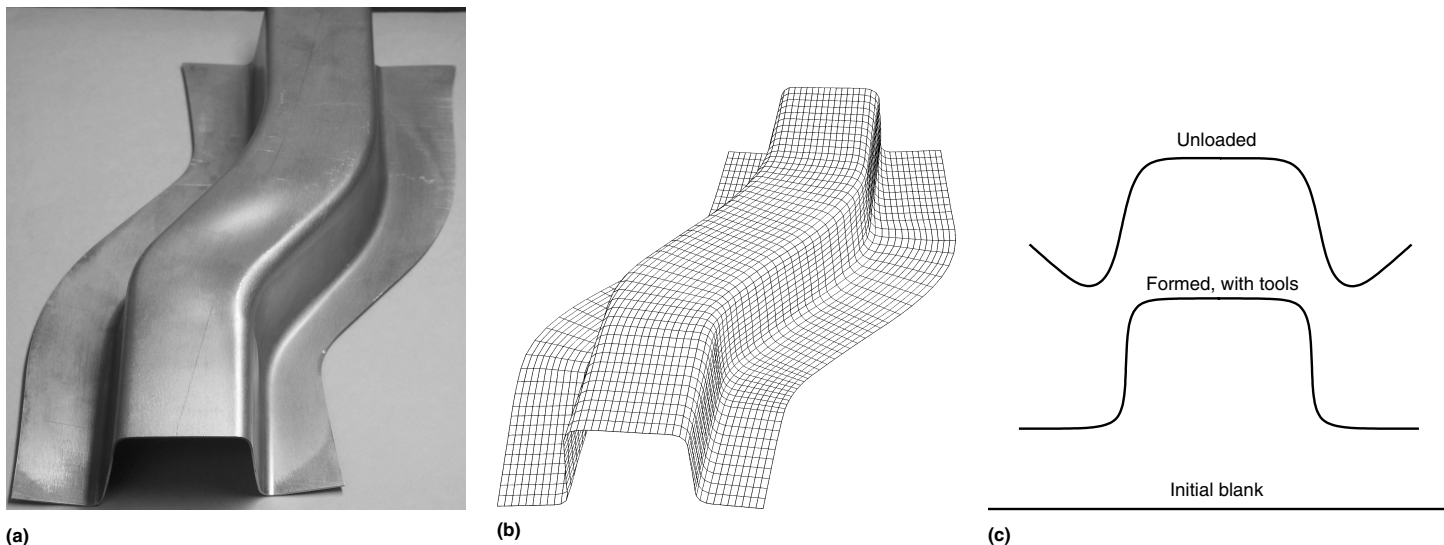


Fig. 1 Typical automotive sheet-formed part, the S-rail. (a) Formed part. (b) Finite element representation, as formed. (c) Cross-sectional schematics at three forming stages. Source: Ref 1

2 / Process Design for Sheet Forming

changes caused by springback can be very significant even though the elastic strains driving the springback can be tiny.

To introduce an applied example, Fig. 1(a) shows a representative automotive formed part referred to as the S-rail (Ref 1). Figure 1(b) depicts a corresponding finite element mesh, and Fig. 1(c) focuses on a schematic cross section of this part at three stages: initial (flat), as-formed (with tools in place), and unloaded (after springback). Inspection of the operation (and ignoring slight stretching at the top web of the part) reveals that the upper corners of the cross section are essentially bent to conform to the punch radius (the punch in this orientation lies below the sheet). When the tooling is removed, these radii open up to larger radii. This is typical of an idealized bending-with-tension operation. The sidewall regions of the formed rail or channel are drawn over the die radii (the die lies above the sheet in this orientation) over large distances, such that each element undergoes bending and unbending sequentially, also under the action of tension. When loaded, the sidewalls are flat. The final shape of the sidewalls incorporates what is known as sidewall curl. The level of tension for each location is related to the binder force, the friction with the tooling, and the work required to bend, unbend, and draw. If a draw bead were involved, this would add yet another element to the sheet tension determination.

The primary focus in this article is on sheet metal forming operations, such as the one shown in Fig. 1. This focus allows conclusions to be drawn with reference to a relatively narrow range of thicknesses and bend radii, both of which are small relative to the width of the body. The equations and results are nonetheless applicable to other geometries, with restrictions specified as necessary.

This article is organized in sections. The subject of springback is first addressed for the simplest, most easily understood cases, that is, pure bending of slender beams or sheets. While such treatments are applicable to few problems of applied interest, their study reveals the principles governing the problem and addresses the limitations of the various assumptions. To these treatments is then added the effect of superimposed tension, which is shown to be a critical variable for accurate prediction of springback. From these generally closed-form treatments, a leap is made to the much more general and practical prediction of springback for real forming operations, using either experience or finite element modeling. Finally, the design of dies and tooling using an assumed springback prediction capability is addressed.

Pure Bending—Classical Results

In order to understand the phenomenon of springback, it is instructive to begin with the simplest case and the most restrictive assumptions. In this section, the case of pure, or simple, bending is considered, that is, bending under

the action of an applied moment without applied sheet tension. The springback consists of assumed elastic unbending on removal of the applied moment.

Assumptions. The assumptions that apply to this case in the simplest treatment may be listed as:

1. Plane sections remain planar.
2. No change in sheet thickness
3. Two-dimensional geometry, either plane strain or plane stress in width direction
4. Constant curvature (i.e., no instability of shape)
5. No stress in the radial, or through-thickness, direction
6. The neutral (stress-free) axis is the center fiber and is the zero-extension fiber.
7. No distinction between engineering and true strain
8. Isotropic, homogeneous material behavior
9. Elastic straining only during springback

The validity of these assumptions is discussed in the next section, but the simple results for springback under these conditions are first presented here.

Within these assumptions, the primary differences among treatments appearing in the literature relate to the assumed material constitutive behavior. There are two basic choices to be made: whether to treat the problem as purely plastic or elastic-plastic, and what form of stress-strain law to adopt in the plastic range. Results have been presented for nearly all choices: perfectly plastic (no hardening), linear hardening (Ref 2), power-law hardening (Ref 3–7), or a general approach (requiring graphical or other numerical integration) (Ref 8, 9).

Basic Equations and Approach. The approach is illustrated in Fig. 2. An initially flat sheet or beam is envisioned. For these purposes, a sheet denotes a part that is very wide relative to its thickness and bend radius and implies that the deformation is nearly plane strain; that is, the strain in width direction is zero. A beam denotes a part that is very narrow relative to thickness and bend radius and implies that the deformation is nearly plane stress; that is, the stress in the width direction is zero. The part is bent to a starting radius (R) under the action of a moment (M). The value of M acting on the sheet or beam is obtained by integrating the stress distribution as:

$$M = \int_{-t/2}^{t/2} \sigma_x(\epsilon_x) z w(z) dz \quad (\text{Eq 1})$$

where ϵ_x is the circumferential strain, σ_x the circumferential stress (Fig. 2b), t is the sheet thickness, and $w(z)$ is the width of the sheet, which in general may vary with the z -coordinate (that is, the cross section need not be rectangular). Assuming a rectangular cross section, taking advantage of the symmetry of the problem (assumptions 6 and 8 in the section “Approximations in Classical Bending Theory” in this article), and substituting into Eq 1 obtains the moment per unit width (M/w), which may be expressed more simply:

$$\frac{M}{w} = \int_{-t/2}^{t/2} \sigma_x(\epsilon_x) z dz = 2 \int_0^{t/2} \sigma_x(\epsilon_x) z dz \quad (\text{Eq 2})$$

The strain shown in Eq 1 and 2, ϵ_x , depends on z . Within the given assumptions, the circumfer-

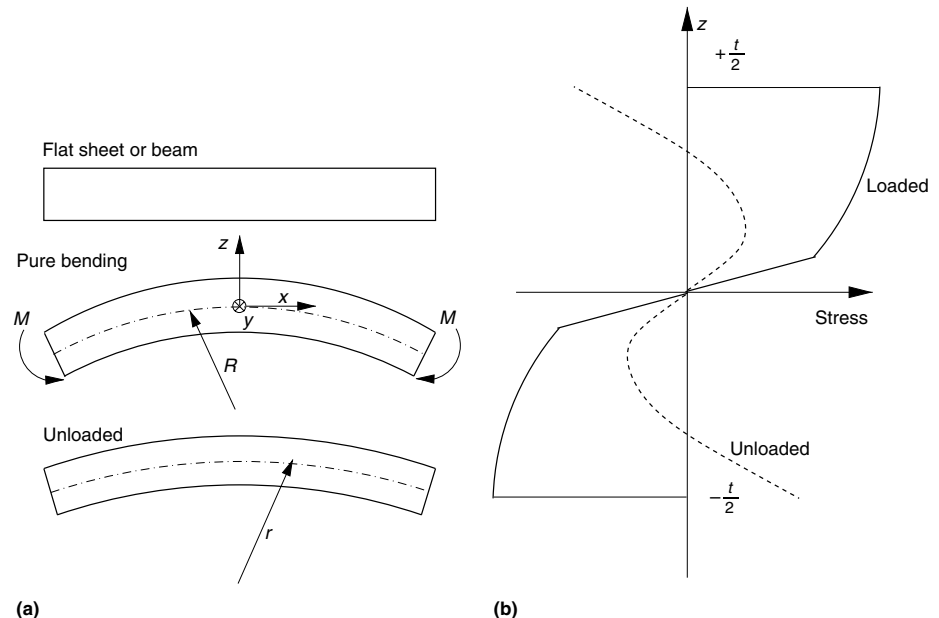


Fig. 2 Schematics of pure bending. (a) Configurations with coordinates defined. (b) Through-thickness stress distribution

Springback / 3

ential strains (ϵ_x) are linearly related to the distance from the center of the sheet (z) and inversely to the bend radius (of the center fiber of the body) R :

$$\epsilon_x \approx e_x = \frac{z}{R} \quad (\text{Eq 3})$$

where it is assumed that the true strain (ϵ_x) and the engineering strain (e_x) are small enough to be used indistinguishably. As is shown explicitly, the bending moment can be calculated using Eq 2 and 3, along with a constitutive relationship between stress and strain.

Note: In order to simplify the notation, the subscript x is dropped from the terms σ_x and ϵ_x , with the understanding that these represent the principal components of stress and strain normal to the beam or sheet cross section (as labeled in Fig. 2).

In order to compute the springback after bending, the moment per unit width of sheet, M/w , is removed from the sheet or beam while the material responds elastically. Because elastic stresses and strains can be superimposed, an alternative view of this operation is obtained by applying a moment (M) to the stress-free body in the configuration of the bent beam or sheet. An isotropic linear elastic beam or sheet has a constitutive response of $\sigma_x = E'\epsilon_x$, where E' is the effective modulus for the beam (plane-stress case) or $E' = E/(1-\nu^2)$, where ν is Poisson's ratio, for the sheet (plane-strain case).

For elastic recovery from an initially curved configuration (radius = R) to a final configuration (radius = r), the relationship for a body of general cross section is:

$$\frac{1}{R} - \frac{1}{r} = \frac{M}{E'I} \quad (\text{Eq 4})$$

where I is the moment of inertia of the cross section.

Note: The springback results for plane strain and plane stress do not differ greatly for most materials. Assuming that the bending moment is proportional to the operative flow stress for an isotropic, nonhardening, von Mises material, the plane-strain bending moment is $2/\sqrt{3}$ (1.15) times the plane-stress moment. Assuming a typical Poisson's ratio of $1/3$, the plane-strain elastic modulus is 1.12 times the plane-stress (i.e., uniaxial tension) one. Thus, the differences between Eq 4 interpreted for plane stress or plane strain is only approximately 1.15 versus 1.12, or approximately a 3% differential. Elastic and plastic anisotropy may change this value.

Moments of inertia may be readily calculated for complex shapes by integration and have been tabulated for a variety of standard structural shapes (Ref 10). For the case of a rectangular cross section, which is assumed in the remainder of this article, the moment of inertia is taken as:

$$I = \frac{wt^3}{12} \quad (\text{Eq 5})$$

where t is the sheet thickness. Equation 4 may be rewritten for a rectangular cross section in a

per-width format as:

$$\frac{1}{R} - \frac{1}{r} = \frac{M}{E'I} = \frac{12M/w}{E't^3} \quad (\text{Eq 6})$$

which may be readily rewritten in the alternate form:

$$\frac{r}{R} = \left[1 - R \frac{M}{E'I} \right]^{-1} = \left[1 - R \frac{12M/w}{E't^3} \right]^{-1} \quad (\text{Eq 7})$$

The form $\left[\frac{1}{R} - \frac{1}{r} \right]$ is called springback in this article, while the second form, r/R , is called the springback ratio. In general, the springback is positive ($r > R$), and the springback ratio is thus greater than unity. The relationship between the two measures is as Springback ratio = $1/(1 - R \cdot \text{Springback})$. For most applications, springback as defined previously is the quantity of interest. For small curvature changes, the shape change displacements are proportional to springback. The springback ratio is occasionally used with some analytical procedures, so a few results in this article are presented using it.

Note that a fractional error associated with the evaluation of springback may be quite different from the fractional error associated with the springback ratio, depending on how large the second term of Eq 7 is relative to 1. That is, when the second term is small, errors of R/r will appear to be small even though the fractional errors on moment can be significant.

Equations 6 and 7 represent the fundamental springback result for pure bending with the assumptions listed. To apply Eq 6, it is necessary to first choose the plane-stress or plane-strain approximation based on width with respect to bend radius and thickness. The bending moment is computed using Eq 2 and 3 and an explicit material stress-strain law (and known stress state). This approach is used to reproduce some classical springback results in the remainder of this section.

Rigid, Perfectly Plastic Result. The simplest springback result for pure bending makes use of a rigid (i.e., no elastic strains), perfectly plastic (no strain hardening) material model (Ref 4–6, 8, 11–13). Under these assumptions, the bending moment (and thus the springback) is independent of the original bend radius:

$$\frac{M}{w} = 2 \int_0^{t/2} \sigma'_0 z dz = \frac{\sigma'_0 t^2}{4} \quad (\text{rigid, perfectly plastic}) \quad (\text{Eq 8})$$

where σ'_0 is the yield stress (also the flow stress) of the material in plane stress or plane strain. The springback, defined here, is obtained using Eq 4:

$$\frac{1}{R} - \frac{1}{r} = \frac{3\sigma'_0}{E't} \quad \text{or, alternatively,} \quad \frac{R}{r} = 1 - \frac{3\sigma'_0 R}{E't} \quad (\text{rigid, perfectly plastic}) \quad (\text{Eq 9})$$

This result is often sufficient for springback prediction, and it reveals the importance of the

principal material properties as they affect springback:

- Springback is proportional to strength/stiffness, that is, σ_0/E .
- Springback is inversely proportional to sheet thickness.

More detailed analysis alters the exact form of these dependencies, but the conclusion remains the same: materials that are strong relative to their elastic modulus are more susceptible to large springback, as are thinner materials. Thus, aluminum sheet of comparable strength to a steel alloy exhibits springback approximately three times greater, because its elastic modulus is approximately $1/3$ as large as that of steel.

Elastic, Perfectly Plastic Result. The first refinement of Eq 9 is by the inclusion of elastic, perfectly plastic bending behavior (Ref 14, 15). That is, there will be an elastic core near the neutral axis. The location of the elastic-plastic transition has a z -coordinate of z^* , which is found by setting the yield strain (σ'_0/E') equal to the bending strain (z/R):

$$z^* = \begin{cases} \frac{R\sigma'_0}{E'} & \text{for } \frac{R\sigma'_0}{E'} \leq \frac{t}{2} \\ & \text{(elastic-plastic case)} \\ \frac{t}{2} & \text{for } \frac{R\sigma'_0}{E'} > \frac{t}{2} \\ & \text{(elastic only, no springback)} \end{cases} \quad (\text{Eq 10a})$$

$$\quad \quad \quad (\text{Eq 10b})$$

Note that the extent of the elastic core is proportional to the bend radius (i.e., inversely proportional to curvature), proportional to the yield stress, and inversely proportional to the elastic modulus. Thus, inclusion of the elastic part of the material response becomes progressively more important for gentle bending of high-specific-strength materials. As is shown later, for typical sheet metal press forming, the bend radius is typically small enough that the elastic region may be neglected without significant loss of accuracy.

Evaluation of the required integral to obtain the moment for elastic-plastic cases may be conveniently split into two terms, the second identical to the rigid, perfectly plastic case outside of the elastic core:

$$\frac{M}{w} = 2 \int_0^{z^*} \frac{E'z}{R} z dz + 2 \int_{z^*}^{t/2} \sigma'_0 z dz \quad (\text{Eq 11})$$

$$= \frac{2E'z^{*3}}{3R} + \frac{\sigma'_0 t^2}{4} - \sigma'_0 z^{*2}$$

Substituting the relationship for the elastic-plastic location, z^* (Eq 10a), obtains the elastic-plastic moment and springback results:

$$\frac{M}{w} = \frac{\sigma'_0 t^2}{4} - \frac{\sigma'_0^3 R^2}{3E'^2} \quad (\text{elastic, perfectly plastic}) \quad (\text{Eq 12})$$

4 / Process Design for Sheet Forming

$$\frac{1}{R} - \frac{1}{r} = \frac{12M/w}{E't^3} = \frac{12}{E't^3} \left[\frac{\sigma_0'^2 t^2}{4} - \frac{\sigma_0'^3 R^2}{3E'^2} \right]$$

(elastic, perfectly plastic) (Eq 13)

The springback equation may be rewritten in an alternate form presented by Gardiner (Ref 14) using Eq 7:

$$\frac{R}{r} = 1 - \frac{3\sigma_0' R}{E't} + \frac{4\sigma_0'^3 R^3}{E'^3 t^3} = 1 - 3x + 4x^3,$$

where $x = \frac{\sigma_0' R}{E't}$ (Eq 14)

Note that the left side of Eq 14 is the reciprocal of the springback ratio as defined in this article. The error introduced by ignoring the elastic core in springback calculations may be evaluated by comparing Eq 9 and 13 or, equivalently, Eq 8 and 11. Table 1 presents R/t ratios where the moment error is limited to 1, 2, 5, and 10%. For a given desired level of accuracy, the R/t ratio is the largest one that can be safely considered.

Typical R/t ratios for automotive press forming lie in the range of 5 to 25, although many examples outside of that range may be found, particularly with general three-dimensional shapes that are not amenable to simple analysis. The results in Table 1 show that ignoring the elastic core leads to very small errors in this range for normal materials (aluminum alloys with a yield stress of 500 MPa, or 73 ksi, are seldom suitable for complex press forming).

Rigid, Strain-Hardening Results. In addition to the results presented previously, bending moments and springback relationships for strain-hardening material models have been presented in various forms, including the following selections:

- Empirical forms (Ref 16)
- Rigid, arbitrary hardening (Ref 8)
- Rigid, power-law hardening (Ref 3-7)
- Rigid, linear hardening (Ref 2)

Power-law hardening models are frequently used for sheet forming analysis. The hardening law, often attributed to Hollomon (Ref 17), may be written as follows, in uniaxial stress and other fixed stress- or strain-ratio forms:

$$\begin{aligned} \sigma &= K\varepsilon^n \text{ (uniaxial stress) } \text{ or} \\ \sigma' &= K'\varepsilon'^n \text{ (general stress state) } \end{aligned} \quad \text{(Eq 15)}$$

where K is the strength parameter, K' is the effective strength parameter, n is the strain-hardening index, and the primes indicate that the strains and stresses to be considered must take into account the stress-strain state and the form of the yield function (anisotropic, quadratic, etc.). (Because elasticity is ignored, ε is the total strain, equal to the plastic strain.) Typical results for such hardening may be summarized as (Ref 6):

$$\frac{M}{w} = \left(\frac{2}{n+2} \right) \frac{K'}{R^n} \left(\frac{t}{2} \right)^{n+2} \quad \text{(Eq 16)}$$

$$\frac{1}{R} - \frac{1}{r} = \left(\frac{6}{n+2} \right) \frac{K'}{E't} \left(\frac{t}{2R} \right)^n \frac{1}{t} \quad \text{(Eq 17)}$$

Elastic-Plastic Result. Bending moments and springback relationships for elastoplastic, strain-hardening material models have also been presented in various forms, including:

- Elastic, power-law hardening (Ref 18, 19)
- Rigid, linear hardening (Ref 18)

In order to assess the importance of strain hardening in pure bending results, moment and springback formulas were derived based on a hardening law of the following form:

$$\begin{aligned} \sigma &= \sigma_0 + K\varepsilon_p^n \text{ (uniaxial stress) } \text{ or} \\ \sigma &= \sigma_0' + K'\varepsilon_p'^n \text{ (general case) } \end{aligned} \quad \text{(Eq 18)}$$

For the plane-stress case, ε_p signifies the approximate plastic strain, that is, the total strain less the elastic yield strain:

$$\varepsilon_p = \varepsilon - \varepsilon_e \approx \frac{z - z^*}{R} \quad \text{(Eq 19)}$$

The second equality of Eq 19 is approximate because the elastic strain (ε_e) is treated as a constant corresponding to the value at first yield, rather than as evolving with hardening. This approximation, adopted for simplicity, has little effect on the result.

The moment consists of three terms, the first two identical to the elastic, perfectly plastic result, that is, Eq 12 (with yield stress, σ_0), and the third an integral corresponding to the additional moment caused by the hardening beyond the yield stress. This third term may be evaluated as:

$$\frac{\Delta M}{w} = 2 \int_{z^*}^{t/2} K\varepsilon_p^n z dz = \frac{2K}{R^n} \int_{z^*}^{t/2} (z - z^*)^n z dz \quad \text{(Eq 20)}$$

where, as before, $z^* = R\sigma_0/E$. Equation 20 may be evaluated to obtain the explicit form of the incremental moment:

$$\begin{aligned} \frac{\Delta M}{w} &= \frac{2K}{R^n(n+2)} \left(\frac{t}{2} - z^* \right)^{n+2} \\ &+ \frac{2Kz^*}{R^n(n+1)} \left(\frac{t}{2} - z^* \right)^{n+1} \end{aligned} \quad \text{(Eq 21)}$$

The full moment for the elastic, hardening plastic case is thus:

$$\begin{aligned} \frac{M}{w} &= \frac{\sigma_0 t^2}{4} - \frac{\sigma_0^3 R^2}{3E^2} + \frac{2K}{R^n(n+2)} \left(\frac{t}{2} - z^* \right)^{n+2} \\ &+ \frac{2Kz^*}{R^n(n+1)} \left(\frac{t}{2} - z^* \right)^{n+1} \end{aligned} \quad \text{(Eq 22)}$$

and the springback is then:

$$\frac{1}{R} - \frac{1}{r} = \frac{12M/w}{Et^3} \quad \text{(Eq 23)}$$

where M is given by Eq 22.

Springback based on Eq 23 is compared in Fig. 3 with springback computed analytically using elastic, perfectly plastic material behavior (Eq 13), rigid, perfectly plastic material behavior (Eq 9), and elastic-plastic finite element (FE) simulations of four-point bending (Fig. 4). (Finite element simulations are introduced later in this article, but are included here for completeness. The FE results presented in Fig. 3 were verified by refining meshes and number of integration points until no significant changes were observed.) The FE simulations make use of either plane-stress quadratic solid elements (labeled CPS8) or plane-stress beam elements with shear terms (labeled B21). The element labels correspond to the ABAQUS (Ref 20) elements used.

For purposes of Fig. 3 and subsequent use in this article, two material models corresponding to ratios of extremes of yield stress (σ_y) to Young's modulus for typical forming materials were defined based on Eq 18. The soft material, low-strength steel, is based on properties appearing in the literature (Ref 21) for interstitial-free steel: yield stress is 150 MPa (22 ksi), ultimate tensile strength is 310 MPa (45 ksi), and uniform elongation is 28.5%. The hard material, high-strength aluminum, is based on the properties appearing in the literature (Ref 22) for 7075-T6: yield stress is 500 MPa (73 ksi), ultimate tensile strength is 572 MPa (83 ksi), and uniform elongation is 11%.

Parameters of Eq 18 can be determined from the yield stress, ultimate tensile strength, and uniform elongation by noting two conditions: 1) the engineering stress at the uniform elongation is equal to the ultimate tensile strength (σ_{UTS}), and 2) the derivative of the true stress/true plastic strain equation is equal to the true stress at the uniform elongation (σ_f) (or corresponding plastic true strain, ε_f^p). Use of these two conditions, and associating σ_0 of Eq 18 with the yield stress, σ_y , allows determination of the parameters of Eq 18

Table 1 Maximum ratios of bending radius to thickness (R/t) for specified moment errors by neglecting the elastic core in bending (perfectly plastic)

Material	Yield stress		Young's modulus		Maximum R/t for moment error of:			
	MPa	ksi	GPa	10 ⁶ psi	1%	2%	5%	10%
Low-strength steel	150	22	210	30	85	120	190	270
Low-strength aluminum	150	22	70	10	28	40	64	90
High-strength steel	500	73	210	30	26	36	57	81
High-strength aluminum	500	73	70	10	9	12	19	27

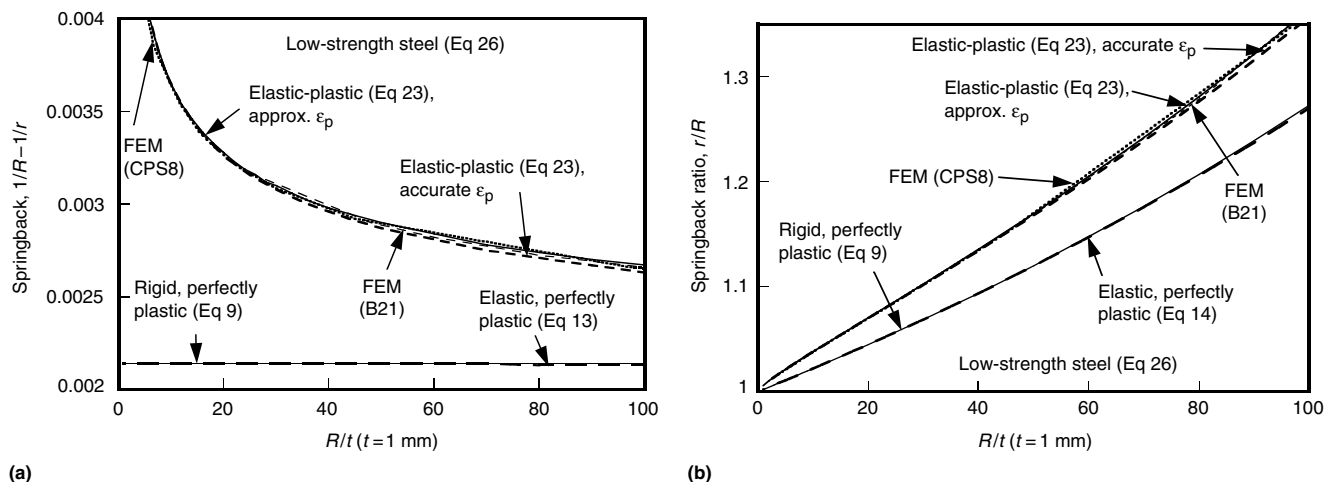


Fig. 3 Effect of various approximations (Eq 9, 13, 14, 23, and 26) on simulated springback quantities. (a) Springback. (b) Springback ratio. R , radius of primary bending curvature; r , radius of curvature after springback; ϵ_p , plastic strain; FEM, finite element modeling; t , thickness. CPS8 and B21 are ABAQUS 6.2 element designations. Source: Ref 20

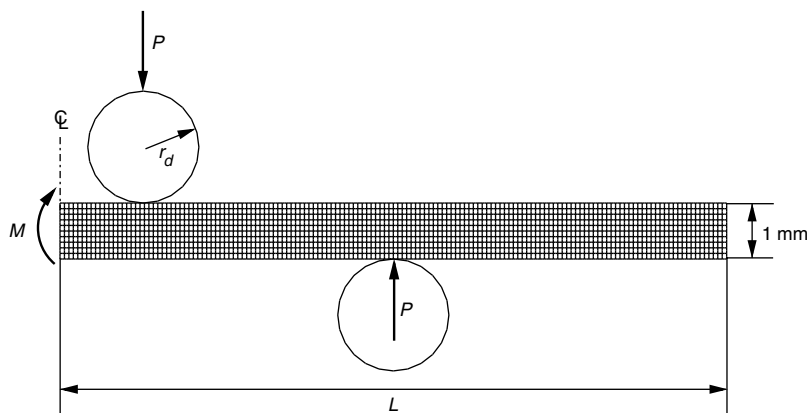


Fig. 4 Finite element modeling (FEM) mesh (CPS8 plane-stress solid elements shown) and tools for simulation of pure bending. M , bending moment; P , applied load in four-point bend FEM; r_d , tool radius in four-point bend FEM; L , half-sample length. Source: Ref 20

as follows:

$$n = \frac{\sigma_f}{\sigma_f - \sigma_y} \epsilon_f^p \quad (\text{Eq 24})$$

$$K = \frac{\sigma_f - \sigma_y}{(\epsilon_f^p)^n} \quad (\text{Eq 25})$$

For the two chosen materials, explicit elastic-plastic constitutive equations are:

Low-strength steel:

$$\sigma = 150 \text{ MPa} + 425 \text{ MPa} \epsilon_p^{0.4}, E = 210 \text{ GPa} \quad (\text{Eq 26})$$

High-strength aluminum:

$$\sigma = 500 \text{ MPa} + 400 \text{ MPa} \epsilon_p^{0.45}, E = 70 \text{ GPa} \quad (\text{Eq 27})$$

As illustrated in Fig. 3(a) neglecting strain hardening leads to large errors in springback throughout the range of R/t tested, varying from

approximately 20 to 50%. (The smaller fractional error for springback ratio is illustrated in Fig. 3b.) For pure bending, Eq 23 is in good agreement with the FE results, whether or not the strain distribution through the thickness of the sheet is approximated.

Approximations in Classical Bending Theory

In this section, the assumptions introduced previously are discussed and, in some cases, evaluated semiquantitatively. As is shown throughout this article, the most important aspects for accuracy in springback prediction for typical sheet forming operations (R/t assumed to be in the range of 5 to 25) involve:

- Sheet tension (most critical aspect, presented in the next section)

- The hardening law (discussed in the previous and last sections)
- Presence of anticlastic curvature (this section and the last)

The basic assumptions of the previous section for pure bending have fairly small errors associated with them. However, these errors can grow when elastic-plastic laws are considered and when bending and unbending occur. It is useful to consider first the effect of the various approximations made within the foregoing pure-bending analysis.

Assumption 1: Plane Sections Remain Planar. For bending and bending under tension, this assumption is very nearly satisfied under most circumstances. For $R/t \geq 5$, shell finite elements (which incorporate this assumption, among others) agree well with full solid elements, which allow general deformation patterns (see later section of this article). Therefore, for $R/t > 5$, the assumption degrades the accuracy little. Another indicator is the accuracy of more complicated closed-form solutions for pure bending. These solutions (Ref 4, 5, 19, 23) retain the planar section assumption but allow through-thickness stresses to develop. These solutions are in good agreement with experiments for small R/t , thus indicating again that the assumption of planar sections has little effect on pure bending over a wide range of R/t .

There are two circumstances where this assumption may be significantly violated: when the frictional stress of sliding on the inner surface of the part is significant relative to bending and stretching forces, and when the hardening law is such that instabilities can occur (assumption 4 in this section). For pure bending and bending under tension (i.e., without frictional contact), the assumption of plane sections remaining plane is reasonable for most situations, probably down to R/t ratios as small as 1.

6 / Process Design for Sheet Forming

Assumption 2: No Change in Sheet Thickness. This assumption is related intimately with pure bending, for which it is very accurate, even to small R/t ratios. Thick shell results (Ref 23, 24) show this directly, although for R/t ratios less than 1, some thickness changes can occur (Ref 25). The use of the phrase “thick shell” in this article refers to a relaxation of some thin-shell approximations. This is distinct from the specialized use of this phrase in the mechanics literature to refer to a particular, systematic development of the kinematics of shell theory. For bending under tension, as presented in the next section, the thickness change is marked.

Assumption 3: Two-Dimensional Geometry, Either Plane Strain or Plane Stress in Width Direction. This is not a good assumption for many bending operations. As illustrated in Fig. 5, as bending occurs in the principal axis, a curvature develops across the width of the specimen. The effect is well known (Ref 26, 27).

The origin of this anticlastic curvature is easily understood: the principal bending causes lengthening of fibers above the neutral axis and shortening of those below it. For lengthened fibers there are Poisson contractions in the width and thickness directions, while for the shortened fibers there are expansions. Across the entire thickness, for pure bending, these very nearly balance each other, hence assumption 2 (no change in sheet thickness) is very accurate under most circumstances.

When the width changes are considered, the tendency to develop a secondary curvature is clear. The outer fibers tend to contract laterally and the inner ones to expand, so a concave-up curvature is favored. For very wide geometries (relative to thickness and bend radius), the plane-strain assumption becomes the limiting case (although there will always be some anticlastic curvature near the sheet edges). For narrow geometries, the anticlastic curvature is unimpeded by shear terms, and the cross section adopts a circular shape with radius of curvature $R_a = \nu/R$ (Ref 9). The plane-stress assumption is the limiting case when there are no stresses resisting the adoption of this shape.

For pure-elastic bending, the shape of the cross section has been found analytically (Ref 28), and a literature review of the subject has appeared (Ref 29). In spite of the limited accuracy of the result for small R/t (the inaccuracy arises by considering the bent configuration to be parabolic), the results are illuminating for typical sheet-forming cases.

The most important result is that the configuration of the bent part is determined by a single dimensionless parameter (β) describing the normalized width (w) of the specimen, sometimes called Searle’s parameter (Ref 30, 31):

$$\beta = \frac{w^2}{Rt} = \frac{w}{R} \cdot \frac{w}{t} \quad (\text{Searle's parameter}) \quad (\text{Eq 28})$$

along with the Poisson’s ratio, ν . The actual shape of the cross section for various values of β is illustrated in Fig. 6, where the bend radii

are also shown assuming a fixed width of 50 and unit thickness of 1. The results in Fig. 6 correspond to the analytic solution as follows, where C_1 and C_2 are numerical constants:

$$\left(\frac{z}{t}\right) = C_1 \cosh\left(\frac{y\alpha}{w}\right) \cos\left(\frac{y\alpha}{w}\right) + C_2 \sinh\left(\frac{y\alpha}{w}\right) \sin\left(\frac{y\alpha}{w}\right) \quad (\text{Eq 29})$$

$$\text{where } C_{2,1} = \frac{\nu}{\sqrt{3(1-\nu^2)}} \times \frac{\sinh\left(\frac{\alpha}{2}\right) \cos\left(\frac{\alpha}{2}\right) \pm \cosh\left(\frac{\alpha}{2}\right) \sin\left(\frac{\alpha}{2}\right)}{\sinh(\alpha) + \sin(\alpha)}$$

$$\text{with } \alpha = \sqrt[4]{3(1-\nu^2)}\sqrt{\beta}.$$

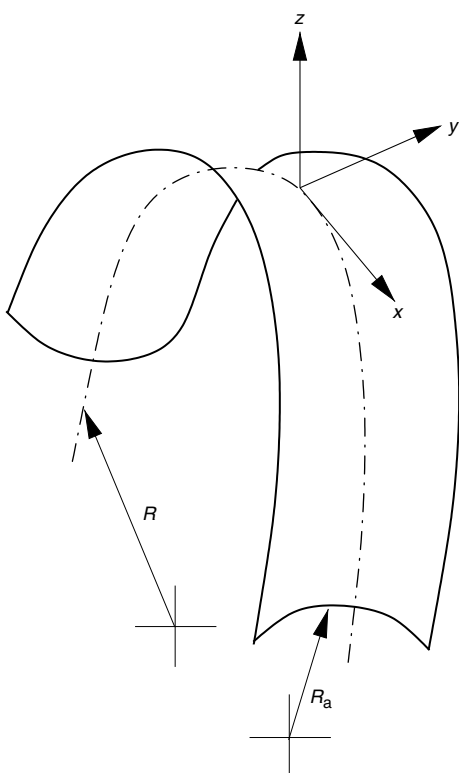


Fig. 5 Anticlastic surface with two orthogonal curvatures. R , radius of primary bending curvature; R_a , radius of anticlastic curvature.

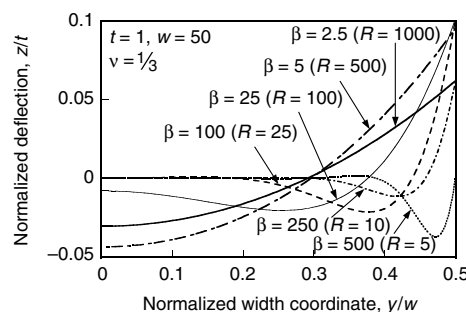


Fig. 6 Shape of cross sections for various values of Searle’s parameter, $\beta = (w^2/Rt)$. z , thickness coordinate; t , sheet thickness; y , width coordinate; w , sheet width; ν , Poisson’s ratio; R , radius of primary bending curvature; β , Searle’s parameter

For β greater than approximately 100, the edge regions look similar and the center region is essentially flat, thus implying that plane-strain conditions are accurate except at the local edge regions. For small β , the cross-sectional shape is essentially circular, which implies that the stresses resisting this curvature may be safely ignored (i.e., plane stress).

The transition from the plane-stress limit to the plane-strain limit is a smooth function of β , as shown in Fig. 7. The limiting values of β for specified errors of the effective moment of inertia are shown in Table 2.

For springback application, the most important effect of anticlastic curvature is two-fold: on the bending moment-curvature relationship, and on the elastic unloading response. The latter will depend greatly on the degree to which the anticlastic shape persists, that is, how much of the anticlastic shape is retained after unloading. For the case of pure-elastic bending and unloading, there is no difference in springback, that is, zero springback, for cases with or without anticlastic effects. Persistent anticlastic curvature is particularly important for the typical sheet-forming case bending and unbending, as is discussed in the last section of this article. For parts curved in three dimensions, the anticlastic curvature may manifest itself as wrinkling, twisting, or generalized distortion. See, for example, the wrinkled area of the S-rail (Fig. 1a).

Assumption 4: Constant Curvature (i.e., No Instability in Shape). This is closely related to assumption 1. For bending and bending under tension, instabilities can occur because of shear

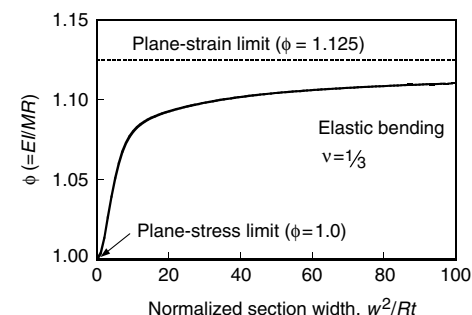


Fig. 7 The transition from the plane stress to plane strain, as a function of $\beta = (w^2/Rt)$. ϕ , anticlastic factor; E , Young’s modulus; I , moment of inertia; M , bending moment; R , radius of primary bending curvature; w , width; t , thickness; ν , Poisson’s ratio

Table 2 Limiting values of β (w^2/Rt) for specified accuracy limits using plane-stress or plane-strain bending formulas

β limit	Limiting value of β for an accuracy limit of:			
	1%	2%	5%	10%
Plane stress ($\beta <$)	2	3	5	34
Plane strain ($\beta >$)	170	42	7	2

banding, for example. These instabilities are expected to be of a similar magnitude and importance and in the same range of strains as for tension or compression. Therefore, when a stable hardening law is obtained (without serrated yielding, Lüder's banding, or yield-point phenomenon), bending may be assumed to behave similarly.

Assumptions 5, 6, and 7: No Stress in the Radial, or Through-Thickness, Direction. The Neutral (Stress-Free) Axis is the Center Fiber and is the Zero-Extension Fiber. No Distinction between Engineering and True Strain. These three assumptions are closely related and may be considered together naturally. To consider these effects profitably, it is simpler to ignore, for the moment, anticlastic curvature. Each of these assumptions is closely related to the R/t ratio to which a flat beam or plate is bent initially. The effect of bending to R/t less than approximately 5 produces significant through-thickness stresses in the interior of the body and causes the stress-free axis to vary significantly from the zero-extension fiber. Bending to small R/t also produces large strains at the outer fibers, thus making the distinction between true and engineering strains more significant (Ref 32).

The last of these effects is the simplest to quantify. In order to do so, consider the elastic-plastic result of Eq 20, but this time evaluate the strains in terms of true strains, that is:

$$\epsilon_p = \epsilon - \epsilon_e \approx \ln\left(1 + \frac{z}{R}\right) - \ln\left(1 + \frac{z^*}{R}\right) \quad (\text{Eq 30})$$

Note that again the additional elastic strain that accrues with strain hardening after the elastic-plastic transition point has been ignored. This allows Eq 20 to be rewritten as:

$$\begin{aligned} \frac{M'}{w} &= 2 \int_{z^*}^{t/2} K \epsilon_p^n z \, dz \\ &= 2K \int_{z^*}^{t/2} \left[\ln\left(1 + \frac{z}{R}\right) - \ln\left(1 + \frac{z^*}{R}\right) \right]^n z \, dz \end{aligned} \quad (\text{Eq 31})$$

where, except for the use of true strains, all the other assumptions remain the same. Evaluation of Eq 31 shows that the error on M introduced by neglecting true strain is 3.8% for $R/t = 1$ and less than 0.64% for $R/t \geq 5$. Therefore, other assumptions introduce larger errors than this one. (Note that a true kinematical description of bending, whether finite or infinitesimal, is not used for any derivations here. Only the evaluation of strain differs.)

The remaining assumptions related to small R/t can be assessed by the thick-shell solutions for rigid, perfectly plastic behavior presented first by Hill (Ref 33) and later in simplified forms (Ref 4, 5) and less restrictive forms for elastic-plastic cases (Ref 19). The conditions found to hold even during bending to small R/t are plane strain (assumed) and no thickness change.

Maintaining these conditions during bending to small R/t requires consideration of the quadratic terms in the value of the circular arc. The results show that significant through-thickness stresses develop and the stress-free fiber is no longer the zero-extension fiber. The details of the derivations may be found in the references provided, but the general result is that the total true strain for the more precise form is given by:

$$\epsilon = \ln \left[1 + \left(\frac{t}{2R} \right)^2 + \left(\frac{2z}{R} \right) \right]^{1/2} \quad (\text{Eq 32})$$

and the plastic problem must be solved incrementally in order to determine the stress distribution throughout the plastic deformation.

Figure 8 illustrates the relative magnitude of the various approximations for pure bending. The deviations are quite small for the pure bending case.

Assumption 8: Isotropic, Homogeneous Material Behavior. For fixed stress state (plane stress, for example) or strain state (plane strain, for example), the introduction of anisotropy, elastic and plastic, makes no fundamental change in the treatment of two-dimensional bending and springback results. While an extensive treatment of anisotropy is beyond the scope of this article, a simple result can illustrate the general procedure. For more complicated cases, FE analysis is usually required, and FE programs usually have capabilities incorporating material anisotropy.

It is important to note that anisotropy does not affect the basic equations for the simple bending case. For the plastic bending, the relationship between tensile strain at a given fiber and the fiber location (Eq 3) is independent of anisotropy. The relationship between the normal principal stress (σ_x) and the bending moment (Eq 2) is also unchanged. For the elastic unloading, the relationship governing the change of curvature remains the same, except that the modulus is the effective one relating tensile strain (ϵ_x) to normal principal stress (σ_x), taking anisotropy into account.

The role of anisotropy may be reflected sufficiently in a generalized elastic relationship:

$$\sigma_x = E' \epsilon_x = f_E E \epsilon_x \quad (\text{elastic}) \quad (\text{Eq 33})$$

where E' is the effective modulus for the given strain-stress state, and f_E is a constant factor equal to E'/E .

For the plastic relationship, it should be noted that strain hardening is usually specified in terms of effective strain ($\bar{\epsilon}$) and stress ($\bar{\sigma}$) based on a tensile test:

$$\bar{\sigma} = f(\bar{\epsilon}) \text{ for example } \bar{\sigma} = K \bar{\epsilon}^n \quad (\text{Eq 34})$$

Using similar notation, the constant factor reflecting plastic anisotropy and stress-strain state may be defined (Ref 34, 35):

$$\bar{\epsilon} = f_\epsilon \epsilon_x, \quad \bar{\sigma} = f_\sigma \sigma_x \quad (\text{Eq 35})$$

For any fixed anisotropy and strain-stress state, the values of f_E, f_σ , and f_ϵ may be found and

used to complete the basic bending and springback equation, such as Eq 2 to 4.

As an example, consider a sheet with normal plastic anisotropy according to Hill's quadratic yield function (Ref 33). The factors f_ϵ and f_σ can be derived for a given plastic anisotropy parameter (Ref 34), \bar{r} , as:

$$f_\epsilon = \frac{1 + \bar{r}}{\sqrt{1 + 2\bar{r}}}, \quad f_\sigma = \frac{\sqrt{1 + 2\bar{r}}}{1 + \bar{r}} \quad (\text{Eq 36})$$

The necessary strain-hardening relationship, $\sigma_x(\epsilon_x)$ in Eq 2, may then be found in terms of a measured uniaxial hardening law, $\bar{\sigma} = f(\bar{\epsilon})$:

$$\sigma_x(\epsilon_x) = \frac{\bar{\sigma}}{f_\sigma} = \frac{1}{f_\sigma} f(\bar{\epsilon}) = \frac{1}{f_\sigma} f(f_\epsilon \epsilon_x) = \frac{1}{f_\sigma} f\left(f_\epsilon \frac{z}{R}\right) \quad (\text{Eq 37})$$

The substitution may be illustrated conveniently by taking a particular hardening law, say $\bar{\sigma} = K \bar{\epsilon}^n$:

$$\begin{aligned} \sigma_x &= \frac{K}{f_\sigma} \left(f_\epsilon \frac{z}{R} \right)^n = \frac{K(1 + \bar{r})}{\sqrt{1 + 2\bar{r}}} \left[\frac{1 + \bar{r}}{\sqrt{1 + 2\bar{r}}} \frac{z}{R} \right]^n \\ &= \frac{(1 + \bar{r})^{n+1}}{(1 + 2\bar{r})^{\frac{n+1}{2}}} K \left(\frac{z}{R} \right)^n = K' \left(\frac{z}{R} \right)^n \end{aligned} \quad (\text{Eq 38})$$

where K' represents all of the needed changes. The same procedure may be applied to any strain state, tensile hardening law, and fixed plastic anisotropy.

It should also be noted that an assumption of symmetric yielding in tension and compression has been made. For as-received sheet material, this is usually a reasonably accurate picture of the stress-strain behavior. However, as is discussed in the section, "Applied Analysis of Simple Forming Operations" in this article the hardening behavior can become complex in reverse bending, which is common in many sheet-forming situations. Under these conditions, the Bauschinger effect on strain reversal must be considered. (Strictly speaking, some strain increment reversal can take place in single bending, because the neutral surfaces move relative to the midplane. This effect appears not to have been analyzed and is likely very small in practical cases.)

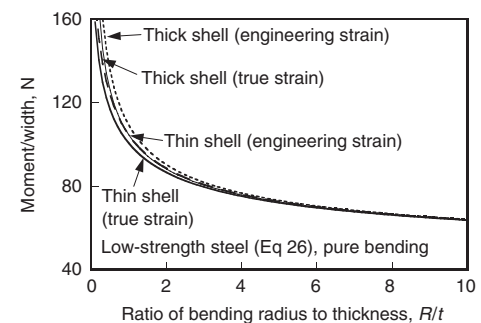


Fig. 8 Comparison of various approximations for elastoplastic pure bending.

8 / Process Design for Sheet Forming

Finally, initial material properties are assumed to be the same at each point in the body.

Assumption 9: Springback Occurs Elastically. For all pure bending and nearly all bending under tension cases, this is very accurate. However, contrary to assertions in the literature (Ref 36), elastic-plastic springback can occur for bending under high sheet tensions (approaching and beyond the yield stress) (Ref 37–40) and when the material behavior is time-dependent (i.e., via creep or anelasticity) (Ref 41, 42). A few examples of such situations are mentioned in the section “Applied Analysis of Simple Forming Operations” in this article.

For most situations, these effects can be ignored without greatly affecting the result. However, it should be noted that unloading itself may involve inelastic effects (Ref 43) that produce changes in the observed modulus (Ref 44). There has been no clear approach on how such effects can be incorporated in springback analysis except for adjusting the effective elastic modulus.

Bending with Tension

The effect of superimposed tension during bending plays a dominant role in determining springback, as is demonstrated with simple analyses. Nearly all sheet-forming operations involve at least some sheet tension, whether introduced by remote sections of the part undergoing deformation, local friction conditions, or the intentional action of a draw bead or other restraint. Increasing sheet tension to reduce springback and its variability has been the principal industrial solution to the problem of inadequate shape fixability.

Analyses similar to those for pure bending can be carried out by relaxing just one of the assumptions listed in the first section, namely the sixth one, that is, that the neutral (stress-free) axis is the center fiber and is the zero-extension fiber. The sheet thickness may change substantially if the tension is high during bending (Ref 45) (and particularly for bending and unbending, which is not considered until the next section), but this effect is often ignored for simplicity. (For FE simulation, in the next section, shell elements usually assume zero thickness change in one time step, but the thickness is updated at the end of each step.)

Springback solutions for bending with tension have been presented with various levels of complexity, including elastic, perfectly plastic (Ref 6–13); elastic, power-law hardening (Ref 18, 19, 46–48); elastic, linear hardening (Ref 18, 49, 50); and rigid, power-law hardening (Ref 51–54). Extension to more complex cases includes: biaxially loaded plates (Ref 36), bending to small radii with tension (Ref 19), the effect on nonsimultaneous tension and bending (i.e., prebending or postbending) (Ref 51), taking into account section changes in narrow strips (Ref 7), the role of nonuniform deformation (Ref 55),

results for laminated sheets (Ref 56), and the effect on formability and residual-stress distribution (Ref 57).

Elastic, Perfectly Plastic Result. The simplest elastic, perfectly plastic solution for bending with tension is sufficient to reveal the dominating importance of tension relative to other variables. Initially considering the thickness constant, the strain distribution through the sheet thickness is a simple superposition of a tensile or membrane strain (ϵ_m) and the bending strain (ϵ_b) as before:

$$\epsilon = \epsilon_m + \epsilon_b = \epsilon_m + \frac{z}{R} \tag{Eq 39}$$

At the neutral axis (assumed to be the zero-extension axis), located at z_0 , the strain is zero, so an expression relating the membrane strain and the neutral axis location is obtained:

$$\epsilon_m = -\frac{z_0}{R} \tag{Eq 40}$$

The stress distribution is similar to the one shown in Fig. 9, which may be integrated to obtain the overall sheet tension, T , (per unit width, w) operating:

$$\frac{T}{w} = \int_{-t/2}^{t/2} \sigma'_0 dz = \int_{-t/2}^{z_0} -\sigma'_0 dz + \int_{z_0}^{t/2} \sigma'_0 dz = -2z_0\sigma'_0 \tag{Eq 41}$$

It is convenient to rewrite Eq 41 in terms of normalized quantities: z_0/t , the fractional location of the neutral axis, and \bar{T} , the average sheet tension stress (T divided by sheet width and thickness) divided by stress to yield the sheet (σ'_0), yielding $\left(\bar{T} = \frac{T}{wt\sigma'_0}\right)$. In terms of these reduced variables, Eq 41 becomes:

$$\left(\frac{z_0}{t}\right) = -\frac{\bar{T}}{2} \tag{Eq 42}$$

With the location of the neutral axis known explicitly in terms of the sheet tension, the moment may be evaluated in closed form:

$$\frac{M}{w} = \frac{\sigma'_0 t^2}{4} [1 - \bar{T}^2], \text{ or} \tag{Eq 43}$$

$$\left(\frac{M/w}{t^2}\right) = \frac{\sigma'_0}{4} [1 - \bar{T}^2] \tag{Eq 44}$$

where Eq 44 emphasizes the proper normalization with thickness. The springback may then be presented in standard and normalized closed forms with the help of Eq 6 and 14 as:

$$\frac{1}{R} - \frac{1}{r} = \frac{12M/w}{E't^3} = \frac{3\sigma'_0}{E't} [1 - \bar{T}^2] \tag{Eq 45}$$

$$\frac{R}{r} = 1 - \frac{3\sigma'_0}{E'} \left(\frac{R}{t}\right) [1 - \bar{T}^2] \tag{Eq 46}$$

Equations 45 and 46 ignore the thickness change that occurs by the action of the sheet

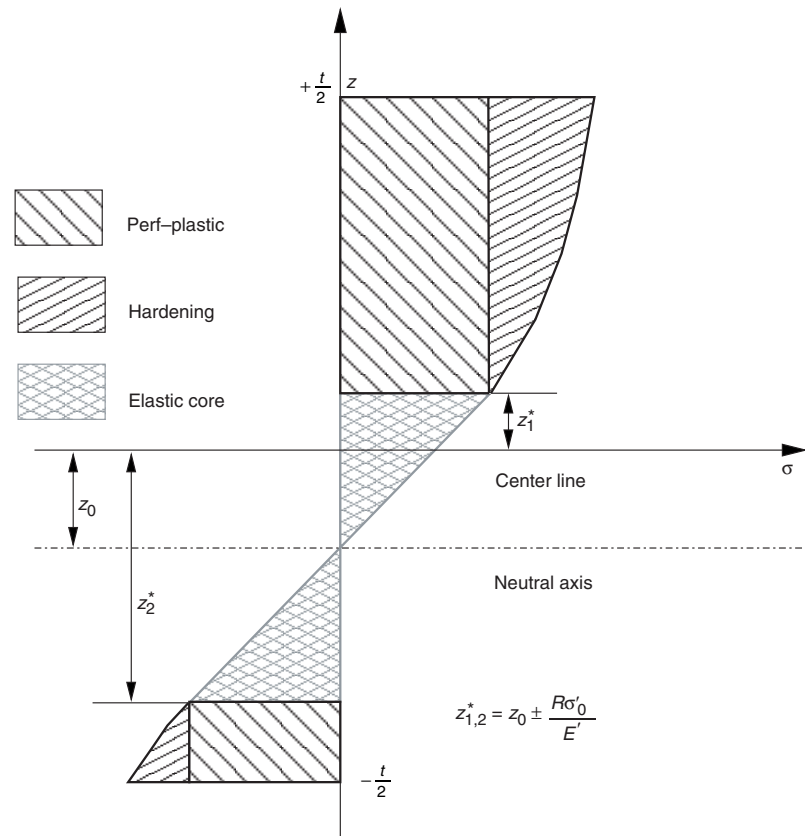


Fig. 9 Schematic of the stress distribution in a beam or sheet, bent to radius R , with definition of various coordinates used in the analysis of springback

Springback / 9

tension; that is, final thickness t is assumed to be equal to original thickness t_0 . The expressions may be approximately corrected for thickness changes by assuming that the final thickness is related to the original thickness such that the volume is maintained using the membrane strain (a linear approximation for the definition of strain is used for simplicity); that is:

$$\frac{t-t_0}{t_0} = -\epsilon_m = \frac{z_0}{R} = -\frac{t\bar{T}}{2R} \quad (\text{Eq 47})$$

where t_0 is the initial thickness, and the final thickness, t , is given by:

$$t = \left(\frac{1}{t_0} + \frac{\bar{T}}{2R}\right)^{-1} \quad \text{or} \quad \frac{t}{R} = \frac{1}{(R/t_0) + \bar{T}/2} \quad (\text{Eq 48})$$

which gives an expression for the final thickness that may be substituted into Eq 45 and 46 to obtain thickness-corrected versions:

$$\frac{1}{R} - \frac{1}{r} = \frac{12M/w}{E't^3} = \frac{3\sigma'_0}{E'R} \left(\frac{R}{t_0} + \frac{\bar{T}}{2}\right) (1-\bar{T}^2) \quad (\text{Eq 49})$$

$$\frac{R}{r} = 1 - \frac{RM/w}{E'I} = 1 - \frac{3\sigma'_0}{E'} \left(\frac{R}{t_0} + \frac{\bar{T}}{2}\right) (1-\bar{T}^2) \quad (\text{Eq 50})$$

The results represented by Eq 46 and 50 are shown graphically in Fig. 10. As can be seen readily, the application of sheet tension substantially reduces springback. For the perfectly plastic case, springback disappears when the normalized sheet tension approaches unity, that is, when the average tensile stress approaches the appropriate yield stress. By setting $\bar{T} = 0$, the pure bending result (Eq 9, for example) is obtained.

Rigid, Power-Law Hardening Result. Using the approach followed previously, the springback predicted for bending with tension can be derived. Unfortunately, it is not in a form as convenient as for the perfectly plastic case. The

only additional complexity is that t cannot be found explicitly in terms of \bar{T} , so that M cannot be written as an explicit function of \bar{T} . It is simplest to proceed by choosing R/t_0 and z_0/t_0 as independent variables, then evaluating the sheet tension, bending moment, and thus springback. In this way, springback may be obtained as a function of sheet tension but not in a closed equation form.

A power-law hardening law with a yield stress as in Eq 15 is adopted, and similar assumptions to the ones mentioned previously are made. Because total strain is represented by Eq 39, the stress throughout the sheet thickness is:

$$\sigma = \begin{cases} \sigma'_0 + K'\epsilon^n, & \epsilon > 0 \quad \text{or} \\ \sigma'_0 + K' \left(\frac{z-z_0}{R}\right)^n, & z > z_0 \\ -(\sigma'_0 + K'|\epsilon|^n), & \epsilon < 0 \quad \text{or} \\ -\sigma'_0 - K' \left(\frac{z_0-z}{R}\right)^n, & z < z_0 \end{cases} \quad (\text{Eq 51})$$

where, as was previously done, the plastic strain is approximated by the total strain (evaluated using the linear, small-strain definition) minus the elastic strain at yield. The normalized sheet tension and bending moment increment (beyond perfectly plastic) may then be obtained as:

$$\bar{T} = -2\left(\frac{z_0}{t}\right) + \frac{K'}{(n+1)\sigma'_0} \left(\frac{t}{R}\right)^n \times \left[\left(\frac{1}{2} - \frac{z_0}{t}\right)^{n+1} - \left(\frac{1}{2} + \frac{z_0}{t}\right)^{n+1} \right] \quad (\text{Eq 52})$$

$$\frac{\Delta M/w}{t^2} = K \left(\frac{t}{R}\right)^n \left[\frac{(0.5 + \frac{z_0}{t})^{n+2} + (0.5 - \frac{z_0}{t})^{n+2}}{n+2} - \left(\frac{z_0}{t}\right) - \frac{(0.5 - \frac{z_0}{t})^{n+1} + (0.5 + \frac{z_0}{t})^{n+1}}{n+1} \right] \quad (\text{Eq 53})$$

where the current thickness must be evaluated in terms of z_0 using either the true-strain definition

or the small-strain approximation:

$$\frac{t}{t_0} = \exp\left(\frac{z_0}{R}\right) \approx \left(1 + \frac{z_0}{R}\right) \quad (\text{Eq 54})$$

Equation 53 represents the additional bending moment caused by strain hardening that must be added to the perfectly plastic moment (Eq 43). The springback ratio is then evaluated using Eq 7. The final springback ratio is shown in Fig. 11.

Corrections to the Simple Power-Law Hardening Result. It is possible to obtain more accurate solutions for this case; however, the equations become rather bulky, will usually require numerical evaluation of integrals, and they will differ for each kind of hardening law considered. (In the truly arbitrary case, a numerical integration can be carried out to obtain the appropriate solution.) Nonetheless, it is useful to illustrate the additional terms that can be considered for completeness and estimation of importance (still adopting assumptions 1 and 3).

For large \bar{T} or small R/t (i.e., large strain), the true-strain definition should be used such that the strains no longer vary linearly through the thickness, except approximately:

$$\begin{aligned} \epsilon &= \epsilon_m + \epsilon_b = \ln\left(1 - \frac{z_0}{R}\right) + \ln\left(1 + \frac{z}{R}\right) \\ &= \ln\left(1 - \frac{z_0}{R}\right) \left(1 + \frac{z}{R}\right) \\ &= \ln\left(1 - \frac{z_0}{R} + \frac{z}{R} - \frac{z_0 z}{R^2}\right) \\ &\cong -\frac{z_0}{R} + \frac{z}{R} \left(1 - \frac{z_0}{R}\right) \end{aligned} \quad (\text{Eq 55})$$

Inclusion of the large strain formula via Eq 55 will usually require numerical evaluation of the integrals to obtain \bar{T} and M . Furthermore, bending to large curvatures (R/t less than approximately 5) introduces errors in the other approximations that are more significant than the small strain form (see the section "Approximations in Classical Bending Theory" in this article). Forms equivalent to the last approximate

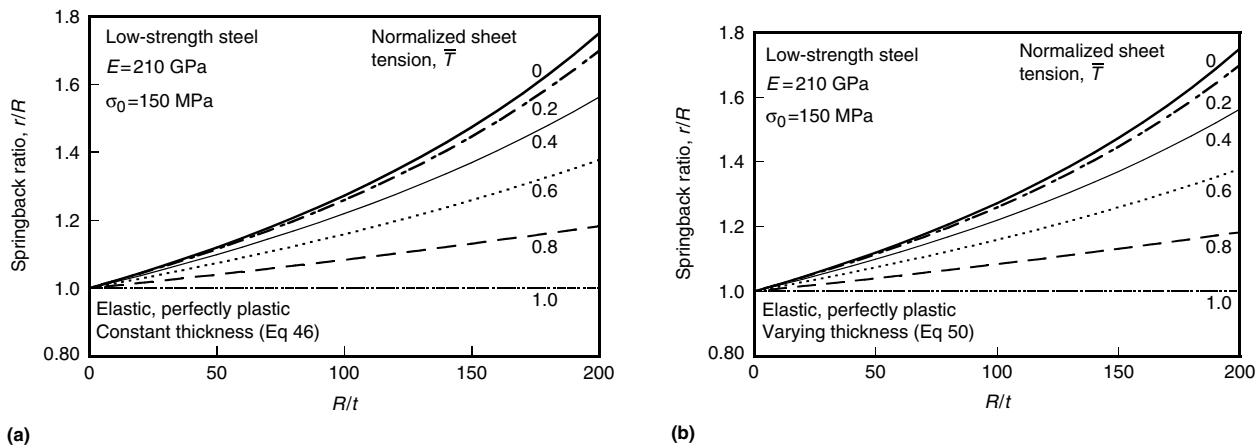


Fig. 10 Effect of sheet tension on springback for an elastic, perfectly plastic constitutive equation for low-strength steel. (a) Constant thickness. (b) Changing thickness. r , radius of curvature after springback; R , radius of primary bending curvature; t , sheet thickness; E , Young's modulus; σ_0 , initial yield stress

10 / Process Design for Sheet Forming

one shown in Eq 55 have been used in the derivations already presented.

Figure 12 shows that the use of true or engineering strain (ϵ_t) has little effect on either the thin-shell or thick-shell solutions. Even at $R/t = 2$, the error is a few percent, and it is inconsequential for $R/t \geq 5$, where the overall approach applies.

The proper plastic strain can be found by subtracting the elastic strain, which depends on the current flow stress of the material:

$$\begin{aligned} \epsilon_p &= \epsilon_t - \frac{\sigma'_f}{E'} = \epsilon_t - \frac{1}{E'} (\sigma_0 + K\epsilon_p^n) \\ &= \epsilon_t - \frac{\sigma_0}{E'} + \frac{K\epsilon_p^n}{E'} \end{aligned} \tag{Eq 56}$$

Equation 56 cannot be rewritten to find ϵ_p explicitly, as required for substitution in the hardening law, but the result may be used nonetheless in evaluating the required integral numerically. Note that the third term on the right side of Eq 56 has been ignored throughout the previous derivations, thus enabling explicit evaluation of ϵ_p from ϵ_t . This has little effect for materials with typical hardening laws (Fig. 13).

For large R/t (small bending strain), the elastic core may make an appreciable contribution to the evaluation of the bending moment. (This was previously illustrated for the nonhardening case.) In this case, the integrals for \bar{T} and M are carried out over only the part of the thickness subjected to plastic strain. The results for hardening can be added to the elastic, perfectly plastic result (e.g., Eq 12) to obtain the full solution, as was illustrated in the previous section for pure bending.

The result for the plastic part of these quantities, say \bar{T} and ΔM , is the same as Eq 52 and 53, with z_0 replaced by z_1^* and z_2^* , where z_1^* and z_2^* are the location of the transitions from elastic to plastic behavior above and below the

neutral axis. That is:

$$\begin{aligned} \bar{T} &= -\frac{2z_0}{t} + \frac{K}{(n+1)\sigma_0} \left(\frac{t}{R}\right)^n \\ &\times \left[\left(\frac{1}{2} - \frac{z_1^*}{t}\right)^{n+1} - \left(\frac{1}{2} + \frac{z_2^*}{t}\right)^{n+1} \right] \end{aligned} \tag{Eq 57}$$

$$\begin{aligned} \frac{\Delta M}{w} &= K \left(\frac{1}{R}\right)^n \\ &\times \left[\frac{(0.5t - z_1^*)^{n+2} + (0.5t + z_2^*)^{n+2}}{n+2} \right. \\ &\left. + \frac{z_1^*(0.5t - z_1^*)^{n+1} - z_2^*(0.5t + z_2^*)^{n+1}}{n+1} \right] \end{aligned} \tag{Eq 58}$$

$$\begin{aligned} \frac{M}{w} &= \frac{2}{3} E' R^2 \left(\frac{\sigma'_0}{E'}\right)^3 + \frac{\sigma'_0}{4} \\ &\times [t^2 - 2(z_1^{*2} + z_2^{*2})] \end{aligned} \tag{Eq 59}$$

Care must be taken using Eq 57 and 58 that z_0 , z_1^* , and z_2^* are not assigned nonphysical values outside of the sheet thickness. That is, the following rules apply to all of the calculations illustrated so far:

$$z_0 = \begin{cases} -\epsilon_m R & -\frac{t}{2} \leq -\epsilon_m R \leq \frac{t}{2} \\ \frac{t}{2} & -\epsilon_m R > \frac{t}{2} \\ -\frac{t}{2} & -\epsilon_m R < -\frac{t}{2} \end{cases} \tag{Eq 60}$$

$$z_1^* = \begin{cases} z_0 + \frac{R\sigma'_0}{E'} & \frac{R\sigma'_0}{E'} \leq \frac{t}{2} \\ \frac{t}{2} & z_0 + \frac{R\sigma'_0}{E'} > \frac{t}{2} \end{cases} \tag{Eq 61}$$

$$z_2^* = \begin{cases} z_0 - \frac{R\sigma'_0}{E'} & z_0 - \frac{R\sigma'_0}{E'} \geq -\frac{t}{2} \\ -\frac{t}{2} & z_0 - \frac{R\sigma'_0}{E'} < -\frac{t}{2} \end{cases} \tag{Eq 62}$$

Evaluation of Eq 58 and 59 (Table 3), shows that for $0 < \bar{T} < 1$, the maximum error caused by neglecting the elastic core is 0.17% ($R/t = 25$) in sheet-forming range and grows to 4.6 and 13.8% for R/t of 100 and 200, respectively.

The foregoing results and discussions show that for the typical sheet-forming regions ($5 < R/t < 25$), the elastic response of the material may be safely ignored, along with more complicated treatments of the strain and thick shells. For large R/t , the elastic strains become significant, and for smaller R/t , the thick-shell approach and proper plastic-strain measures become significant.

Applied Analysis of Simple Forming Operations

For a typical industrial sheet-forming operation, the sheet workpiece is pressed between nearly rigid tools with draw-in constraints enforced, usually via draw beads. The general operation may be arbitrary in three dimensions, and conformance to the tools is by no means assured (Ref 58), thus making it impossible to know, a priori, the bend radius of the sheet. Many material elements undergo bending and unbending with superimposed tension, whereas the closed-form analyses usually assume a flat starting configuration in both in-plane directions. Determining sheet tension, which was shown in the last section to be critically important in springback, is complex, depending on friction, bending and unbending, and boundary constraints. All of these variables may change throughout the part and the forming stroke, over small distances and times.

For arbitrary, three-dimensional (3-D) forming operations, FE analysis (or a similar numerical method) is required throughout the forming operation to obtain a final, as-formed state. This configuration (with tool contact forces) may then be used as a basis for a general springback

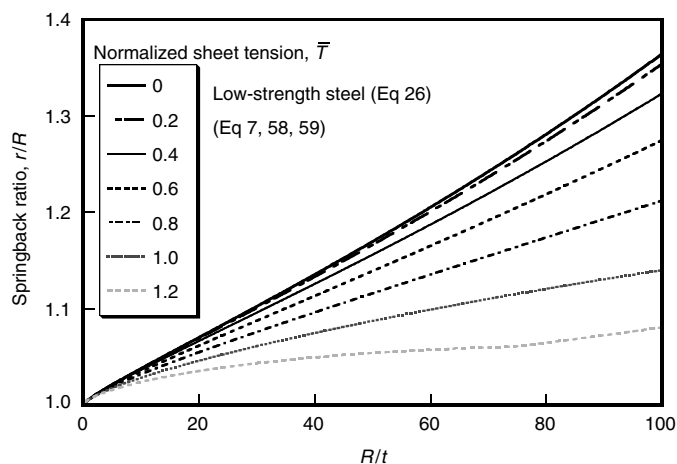


Fig. 11 Role of normalized sheet tension and bend radius on springback for elastoplastic, hardening behavior (Eq 58 and 59) of low-strength steel (Eq 26). See Eq 7, 58, and 59. r , radius of curvature after springback; R , radius of primary bending curvature; t , sheet thickness

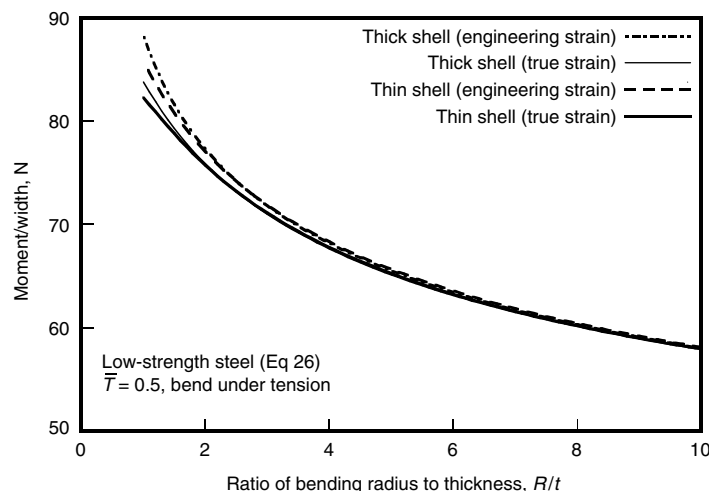


Fig. 12 Comparison of bending moment using thin and thick shells, with either engineering strain or true strain. \bar{T} , normalized sheet tension

analysis using the same, or a different, FE model. Such analysis is discussed subsequently; however, the application of two-dimensional (2-D) closed-form methods is possible and profitable for some classes of forming operations that are first mentioned.

In spite of the difficulties of applied springback analysis discussed previously, certain applied problems have sufficiently restrictive characteristics to provide a basis for closed-form or empirical analysis. Pure bending by dies in two dimensions, for example, may be analyzed using closed-form bending solutions if the work-piece is assumed to conform to the punch surface. Results have been presented for U-bending and V-bending (Fig. 14) using such analysis (Ref 32, 59–63) and empirical approaches (Ref 36, 64–66). A closely related application in sheet metal forming is flanging, for which analysis (Ref 67) and empirical approaches (Ref 68) have been presented.

Closely related operations involving significant tension are often called stretch-bend or draw-bend problems. These operations involve the bending and unbending of sheet as it is progressively drawn over a die. The typical application is often referred to as a top-hat section (Fig. 1c, 15a) and may be called channel forming, among other common names. For large draw-in, the principal springback typically occurs in the form of sidewall curl, which is the curling of the material that was drawn over the die radius (and which was flat while the work-piece was held in the dies during the operation itself). Various analyses based on the methods presented in the last section have appeared (Ref 23, 47–54, 57, 69, 70) and empirical methods have been applied (Ref 71, 72). Such analysis has been extended to consider the differing roles of postbending tension versus prebending tension (Ref 47), laminated materials (Ref 56), and nonuniform bending (Ref 55).

Much of the experimental work appearing in the literature for draw bending must be examined

critically because the tensile stress or load is often not carefully controlled or measured. In a few exceptional cases (Ref 53, 73, 74), direct control was imposed to obtain draw-bend results. For other work, experiments rely on indirect control of tension via friction, draw beads, or die clearances to establish the essentially unknown value of sheet tension. As shown in the last section, the tensile stress has a dominant effect on springback, particularly for values approaching the yield tension, thus leading to large uncertainties in measured results unless the tensile stress is known accurately.

A wide range of experimental data for a draw-bend problem from various sources appears as part of the NUMISHEET '93 *U-Channel Benchmark* (Ref 75). Geometry, material, lubrication, and forming parameters were fully specified by the conference organizers, and numerous laboratories were asked to carry out independent measurements and simulations. The results, shown in Fig. 15(b), illustrate the wide scatter that was obtained. In general, the experimental scatter was greater than or equal to the simulation scatter, illustrating the difficulty in carrying out such experiments with normal industrial forming machinery. It appears that the scatter of experimental results is typical for experiments employing indirect control of sheet tension. The sources of error for the FE simulations are considered in more detail

subsequently, along with a summary of draw-bend results for which the sheet tension is carefully controlled.

Finite Element Analysis

It is only through a complete analysis of the forming operation that the critical variables in springback analysis may be obtained reliably, notably sheet tension, prespringback part shape, distribution of internal properties (such as yield strength), and external loading/internal stresses prior to springback. The geometric complexity of general bodies with curves in three dimensions (such as typical autobody parts, for example) requires discretized treatment. However, finite

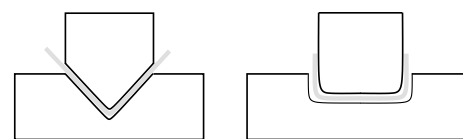
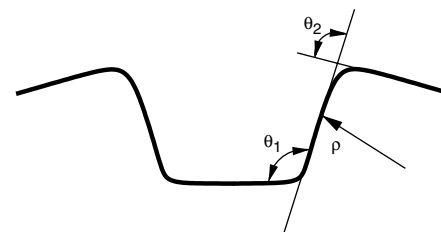


Fig. 14 Schematics of V-bend and U-bend forming operations

Table 3 Maximum error in moment caused by neglecting elastic core for $0 < \bar{T} < 1$, low-strength steel (Eq 26)

R/t	Maximum error in moment, %				
	$\bar{T}=0$	$\bar{T}=0.2$	$\bar{T}=0.5$	$\bar{T}=0.7$	$\bar{T}=1.0$
5	0.002	0.002	0.002	0.002	0.002
25	0.06	0.06	0.06	0.07	0.09
100	1.09	1.12	1.27	1.5	2.4
200	4.8	4.93	5.73	7.04	10.4

R/t, ratio of bending radius to thickness; \bar{T} , normalized sheet tension



(a)

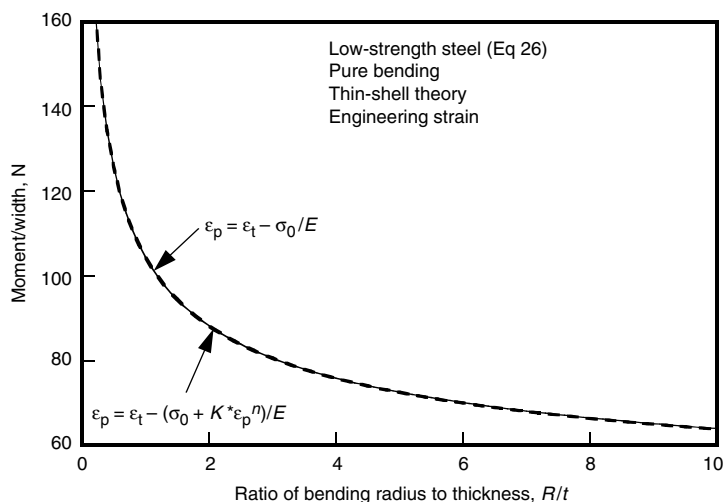
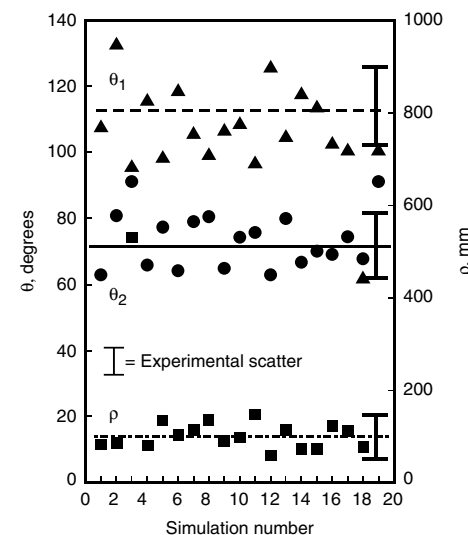


Fig. 13 Effect of strain approximation on springback calculation. See text for definition of variables.



(b)

Fig. 15 U-channel forming and benchmark results. (a) Cross-sectional geometry, after springback. (b) Simulation results (points) and superimposed estimated experimental scatter (bars) for results reported by various laboratories. θ_1 and θ_2 , angles characterizing springback in top-hat samples; p , radius of curvature of sidewall curl

12 / Process Design for Sheet Forming

element analysis (FEA) offers several other advantages as well. Most FE programs readily accept complex laws of material behavior, including anisotropy, elastic-plastic behavior, rate sensitivity, complex hardening, and so on. The more sophisticated programs handle large strain and rotation properly, and arbitrary geometry is treated naturally.

The FEA of sheet forming is well established and now routine (see, for example, various benchmark tests on the subject) (Ref 1, 75–78). The FEA of springback, while appearing to be a simpler problem, requires higher accuracy of both the forming solution and throughout the springback simulation (Ref 39, 41, 79, 80). The choice of element (Ref 38), unloading procedure (Ref 39, 55, 81), and integration scheme (Ref 38, 39, 62, 80, 82, 83) must all faithfully reproduce the stresses and part configuration.

In view of the need for high precision of stress results, implicit forming simulation and implicit springback schemes seem the most likely to succeed (Ref 82). However, claims of success have appeared for nearly every possible combination of procedure: implicit/implicit (Ref 38, 39, 41, 84, 85), explicit/implicit (Ref 79, 82, 83, 86, 87), explicit/explicit (Ref 88, 89), and one-step approaches (Ref 90).

In the section “Draw-Bend Experience” in this article, these general observations are probed with tests and simulations corresponding to draw-in over a die radius in a press-forming operation. In order to understand those results, a brief introduction to the FE method is first presented.

A presentation of the FE method is beyond the ambit of this article. Nonetheless, an understanding of the basic method is helpful in understanding the particular constraints presented by springback analysis following forming analysis.

The following is based on a presentation of FEA particularly aimed at metal forming (Ref 91). Numerous books on the subject of general-purpose FEA have appeared. References 92 to 97 may be of interest for those seeking additional information. They are presented in approximate order of increasing difficulty.

The FE method applied to forming analysis consists of the following steps:

1. Establish the governing equations: equilibrium (or momentum for dynamic cases), elasticity and plasticity rules, and so on.
2. Discretize the spatially continuous structure by choosing a mesh and element type.
3. Convert the partial differential equations representing the continuum motion into sequential sets of linear equations representing nodal displacements.
4. Solve the sets of linear equations sequentially, step forward and repeat.

Items 1 and 2 of this list are of particular importance for springback analysis. For item 1, many choices of material model may be used,

but most forming simulations rely on two basic governing equations: either static equilibrium is imposed in a discrete sense (i.e., at nodes rather than continuous material points), or else a momentum equation in the form of $F = MA$ is satisfied for dynamic approaches.* For nearly all commercial codes used for metal forming, the static equilibrium solutions are obtained with implicit methods that solve for equilibrium at each time step by iteration, starting from a trial solution. Thus, such programs are often referred to as static implicit. Examples of static implicit include ABAQUS Standard (Ref 98) and ANSYS (Ref 99). Forming programs that solve a momentum equation typically use explicit methods that convert unbalanced forces at each time increment into accelerations but do not iterate to find an assured solution. Examples include ABAQUS Explicit (Ref 100) and LS-DYNA (Ref 101).

The choice of element refers to the number of nodes per element, the number of degrees of freedom at each node, and the relationship with the assumed interior configuration (among other things) that define the element type. The nodal displacements are the primary variables to be solved for. A fixed relationship between the displacements of points within the finite element to the displacements of the nodes is assumed. In this way, the continuous nature of the deformation within the element is related to a small number of variables. Of course, the distribution in the element may be quite different from the continuum solution, but this difference can often be progressively reduced by refining the mesh, that is, by choosing finer and finer elements. By comparing the solutions, an adequate mesh size can be determined.

The essence of the FE method, as opposed to other discrete treatments such as the finite difference method, lies in an equivalent work principle. As described previously, the continuous displacements within an element are represented by a small number of nodal displacements (and possibly other variables) for that element. Similarly, the work done by the deformation throughout the element is equated to the work done by the displacements of the nodes and thus are defined equivalent internal forces at these nodes.** The internal work is computed by integrating the stress-strain relation over the volume of the element. This frequently cannot be accomplished in closed form, so certain sampling points, or integration points, inside the element are chosen to simplify this integration. The number and location of integration points may be selected to provide the desired balance between efficiency and accuracy, or between locking and hourglassing, as mentioned subsequently.

For forming and springback analysis, the procedure consists of applying boundary conditions (i.e., the motion of a punch or die, the action of draw beads, frictional constraints, and so on), stopping at the end of the forming operation, replacing the various contact forces

by fixed external forces (without changing the shape of the workpiece), and then relaxing the external forces until they disappear. The last step (or steps) produces the springback shape.

Because the choices of program, element, and procedure usually apply to both the forming and springback steps, it is difficult to separate discussions of accuracy between the two stages. The deformation history established in the forming operation is used in the springback simulation via the final shape, loads, internal stresses, and material properties.

Two choices are of particular importance in forming and springback analysis: the type of solution algorithm/governing equation, and the type of element. These two aspects are discussed as follows.

Explicit and Implicit Programs. The first choice facing one wishing to do forming/springback analysis is the type of program. As noted previously, the two standard choices are a dynamic explicit program or a static implicit program, although several companies have both options available, sometimes even during a single simulation. (Also, there are other variations available, such as dynamic solutions solved implicitly.) Table 4 lists general advantages and disadvantages of the two methods.

Most applied sheet-forming analysis in industry currently uses dynamic explicit methods. The complicated die shapes and contact conditions that occur in complex industrial forming are more easily handled by the very small steps required by the dynamic explicit methods. The stress solutions are of little importance. Often, even simulations that are inaccurate in an absolute sense can be used by experienced die designers to guide sequential modifications leading to improved dies. On the other hand, if a certain set of tools cannot be simulated successfully, that is, with an implicit method that does not converge, the die improvement process is stymied completely.

As is shown in the next sections, springback simulation is much more sensitive to numerical procedure than forming analysis. The reason is simple: springback simulation relies on accurate knowledge of stresses throughout the part at the end of the forming operation. Conversely, forming analysis is primarily concerned with

*It should be noted that nearly all commercial forming operations may properly be considered static. That is, the inertial forces are orders of magnitude smaller than the deformation forces and thus may be safely ignored. The use of dynamic solutions to solve such quasi-static problems is for numerical convenience, with a corresponding loss of accuracy whenever the inertial forces are magnified (by mass scaling, for example). Thus, mass scaling must always be examined to quantify the errors introduced.

**Equilibrium in a weak sense is imposed by requiring that the sum of all such internal forces is zero at each node. Compatibility in a weak sense is automatically satisfied because the common nodes of adjacent elements have a single displacement. These are called weak forms because they do not ensure equilibrium or compatibility throughout the entire body, only at the nodes.

Springback / 13

the distribution of strain within the shape of the part. The shape of the final part is largely determined by the shape of the dies because, near the end of the forming operation, contact occurs over a large fraction of the workpiece. Therefore, the oscillatory nature of the stresses obtained at the end of a dynamic explicit analysis may be unsuited for accurate springback analysis. Poor and uncertain results have been reported (Ref 82).

Developments are currently proceeding in attempts to artificially smooth or damp dynamic explicit forming solutions in the hope of providing a stable base for springback calculations. It is too early to be confident that these approaches will be successful. Certain isolated results can appear promising; however, as is shown later in this section, it is not unusual to obtain fortuitously accurate results in springback analysis. For this reason, great caution should be used in drawing conclusions from a small number of apparently accurate predictions.

The foregoing refers to the drawbacks of a dynamic explicit simulation of a forming operation prior to a springback analysis. The springback simulation itself is also much better suited to implicit methods because the operation is dominated by quasi-static elastic deformation that is computed very inefficiently by dynamic explicit methods. For this reason, implicit springback analysis is often favored even after explicit forming analysis.

It is for these two reasons that static implicit methods are better suited to forming analysis where accurate springback predictions are required. The obvious drawback is the uncertain convergence of current versions of such methods.

Choice of Element. For sheet-forming analysis, two principal kinds of elements are popular, although nearly limitless variations are found within each category. The major choices are solid elements and thin-shell elements.

The simplest to understand is the standard eight-node, trilinear solid element, sometimes called a brick element. (When an element is described as linear or quadratic, it refers to the polynomial order of the shape function, that is,

the mapping equation that relates the motion of the nodes to the motion of the continuous interior points in the element. In a linear element, the displacements of interior points vary linearly with their original positions. Trilinear refers to a shape function that is linear in all three dimensions.) The incompressibility constraint of plastic deformation is readily adapted with this element, and it is used for a variety of structural applications, including bulk forming. The major disadvantage is simple: because many such elements are required through the thickness of the sheet, particularly to accommodate springback analysis, the final number of degrees of freedom for applied problems is enormous and the resulting computation time far beyond today's (2005) computers. Such elements are also typically very stiff in bending, thus making them very poor for springback. One improvement is the use of quadratic or higher-order elements, which have better bending behavior, but which add even more degrees of freedom and further aggravate the overwhelming computational intensity.

Many variations of the standard brick element have been introduced with the goal of enabling use of coarse meshes without locking (non-physically high stiffness in certain modes of deformation). Unfortunately, these numerical corrections often introduce the converse phenomenon of hourglassing (nonphysically low stiffness in certain modes of deformation). New solid elements can balance these problems well, but often at the cost of complexity (Ref 102, 103). Unfortunately, even with elements optimized for coarse meshes, the numbers still overwhelm today's (2005) computers for applied sheet-forming analysis, because very small features must be simulated.

By far, the predominant element used for sheet-forming analysis is the thin-shell element, or simple shell element. One can imagine generating such an element by starting with solid elements and shrinking one dimension to small thickness, a strategy that has been pursued (Ref 104, 105). Unfortunately, this procedure leads to locking, and special integration methods (reduced integration, selective reduced

integration, assumed strain methods, and so on) are then necessary to recover reasonable behavior.

Typical shell elements for sheet forming are based on some version of thin-shell theory, which itself makes assumptions about the strain and stress state throughout the body. They may be triangles or quadrilaterals, although quadrilaterals are more common. There is no real thickness to the elements, so clearances between die faces can be a problem in FE simulations where that aspect is important. Usually, the strain is assumed to vary linearly through the "thickness" of the shell for purposes of evaluating the stresses and work of deformation.* Likewise, through-thickness stresses are usually ignored. The usual procedure introduces two new degrees of freedom at each node corresponding to the slope or local rotation of the material plane at that location.

The advantages of shells for applied sheet forming and springback analysis are so persuasive in today's (2005) computing environment that solids are seldom used except for research or when certain conditions are present. These conditions include critical die clearances, two-sided contact, significant through-thickness stresses, and *R/t* ratios less than 5 to 6. Outside of these cases, shell elements are many times more efficient, and they capture the necessary phenomena in most sheet-forming operations, which are dominated by bending and stretching.

Draw-Bend Experience

The advantages and pitfalls of FEA of springback for many sheet-forming operations are revealed by the draw-bend test (Fig. 16), which closely represents the situation in channel forming (Fig. 14b, 15a) and many other press-forming operations. The advantage of the test is that sheet tension may be closely controlled.

The material in the test is drawn over a round tool under the action of a pulling displacement (and corresponding front force) and resisting force (back force). The workpiece may or may not conform completely to the tool surface when under load; it undergoes bending and then unbending under tension, then rebending under the final unloading when it is released from the fixtures. When released, the drawn length of the strip specimen adopts a final radius of curvature (*r'*). This is precisely analogous to the channel-forming operation, where the pulling displacement is provided by the punch displacement, the back force is provided by a draw bead or frictional resistance over a binder

Table 4 Advantages and disadvantages of static implicit and dynamic explicit finite element programs

Program type	Advantages	Disadvantages
Static implicit	<ul style="list-style-type: none"> ● Known accuracy ● Equilibrium satisfied ● Smooth stress variation ● Elastic solutions are possible ● Unconditionally stable 	<ul style="list-style-type: none"> ● Solution not always assured ● Complex contact difficult to enforce ● Long computer processing times for complex contact
Dynamic explicit	<ul style="list-style-type: none"> ● Solution always obtained ● Simple contact ● Short computer processing times with mass scaling 	<ul style="list-style-type: none"> ● Uncertain accuracy ● Equilibrium not satisfied in general ● Mass scaling introduces error in static problems ● Oscillatory stress variation ● Elastic solutions are difficult and slow ● Conditionally stable

*In the limit of no thickness, and consequently no bending stiffness, a thin-shell element becomes a membrane element. These elements are efficient because they do not require additional degrees of freedom at the nodes, but they are unstable in bending, a common mode for many sheet-forming operations.

14 / Process Design for Sheet Forming

surface, and the final radius of curvature of the drawn section is referred to as sidewall curl. When the drawn distance is sufficiently large, the final springback changes are dominated by the sidewall curl (radius r') rather than the changes in the small region in contact with the tool at the end of the test.

Results of draw-bend tests and parallel FE simulations (Ref 40, 74) form the basis for the following observations.

Numerical Parameters. Finite element sensitivity studies (Ref 38, 39, 106) of the draw-bend test revealed that accurate springback prediction requires much tighter tolerances and closer attention to numerical parameters than does forming analysis. Furthermore, the tighter tolerances must be maintained throughout the forming operation; that is, it is not sufficient to do a coarse forming simulation followed by a precise springback simulation (Ref 82).

Using meshes, tolerances, and numerical parameters typical for forming analysis to analyze the draw-bend test gave nonphysical predictions, including, under some conditions, simulated springback opposite to the direction observed. Figure 17(a) (Ref 38) shows the initial simulations and the final ones (i.e., with appropriate choices of model parameters). A mesh size four times finer along the draw direction was required, combined with a number of integration points ten times larger than normal.

The FE sensitivity results based on the draw-bend test may be summarized as:

- The finite elements in contact with tooling should be limited in size to approximately 5 to 10° of turning angle. This is approximately 2 to 4 times the refinement typically recommended for simulation of forming operations.

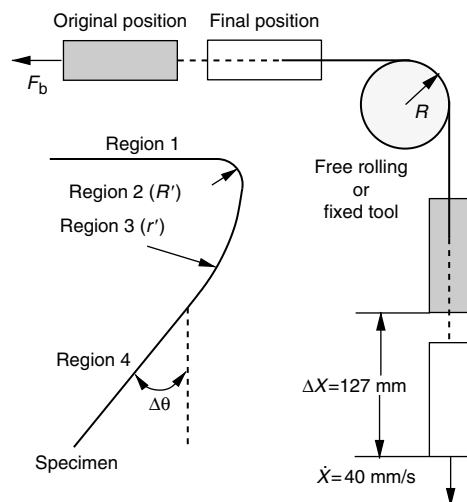


Fig. 16 Schematics of the draw-bend test and final configuration of the unloaded specimen. F_b , normalized back force; R , tool radius; R' , radius of curvature of region in contact with tool, after unloading; r' , radius of curvature in curl region, after springback; $\Delta\theta$, springback angle; ΔX , displacement, the distance between the original and final positions; \dot{X} , displacement rate

- The convergence tolerance and contact tolerance must typically be set tighter than for forming analysis. There are a variety of ways to define such measures, depending on the programs used, so again, the best policy is to refine the measure until the differences become insignificant.
- While most applied sheet-forming analyses use shell elements with three to seven integration points through the thickness, up to 51 integration points are required to assure simulated springback results within 1% of the “converged” solutions. (Converged solutions were obtained by using very large numbers of integration points, until no appreciable change in springback was observed.) More typically, 25 integration points were found to be sufficient for many simulations.

The last of these conclusions represents a dramatic divergence from current practice and remains surprisingly controversial, with researchers continuing to recommend using numbers of integration points ranging from five to nine (Ref 107–111). For this reason, non-FEA numerical studies (Ref 112, 113) were undertaken to explore the errors associated with numerical integration for finite numbers of integration points. Results from the FE sensitivity studies are presented first, then those from the non-FEA numerical studies. The two approaches serve to confirm the main conclusions.

Figure 17(b) (Ref 39) shows a typical result of the FE sensitivity analysis for tests of 6022-T4 aluminum with R/t of 10. In one case, for a normalized back force of 0.9 (relative to the force to yield the strip in tension), 35 integration points were required to meet the 1% tolerance requirement, while for a back force of 0.5, only 21 integration points were required. It is important to note the following points with respect to these results:

- The choice of R/t , back force, and other process and material parameters changes the number of required integration points. However, there is currently no good way to predict the exact number before a simulation is carried out, because many of these quantities are available only after solving the boundary-value problem. As shown subsequently, the effect of process variables on the required number of through-thickness integration points can be determined. Therefore, 25 to 51 integration points are recommended for general cases (if 1% accuracy of springback prediction is desired). As with all FEA, the best policy is to refine the parameters (number of integration points, in this case) to verify that no significant changes take place with continued refinement.
- It is possible, by chance, to obtain accurate results for a given forming problem with a small number of integration points. Note that the results in Fig. 17(b) cross the converged solution several times, with as few as three to five integration points. However, the result

is fortuitous and cannot be assured unless many more integration points are employed. Extrapolating from this result may explain why seemingly rough simulation techniques (such as dynamic explicit solutions, which show oscillatory stress behavior) can produce, with carefully selected (postsimulation) parameters (or sufficient luck!), accurate springback results. The best way to verify the robustness and predictivity of such solutions is by changes of the critical parameters to test whether the solution is a stable one.

- Many 3-D forming operations are much stiffer than the 2-D draw-bend geometry because of the final form of the part. It is unknown what effect this has on the need for numerical accuracy. However, it is clear that for smaller springback, a larger percentage error may be acceptable in terms of the overall geometry changes. Thus, it may not be necessary to demand a 1% springback accuracy; instead, perhaps 10% is adequate. In such cases, the number of integration points may be reduced.

The FEA sensitivity results for the draw-bend test can be understood with the aid of a related but simpler problem: the springback of a beam subjected to an applied R/t and tension force. That is, the state after forming is known analytically, and only the springback is computed, both analytically and numerically. The springback is proportional to the applied moment (Eq 4) so that any fractional numerical error that occurs in evaluating the moment produces a corresponding fractional error in the computed springback. The analytical moment (and springback) may be computed exactly for this problem, and thus, the error induced by the numerical integration scheme during the springback simulation alone can be evaluated separately from other effects. This error is less than the combined errors that can occur during both the forming and springback stages of a simulation.

The following results are extracted from more detailed publications that should be consulted by those seeking more complete information (Ref 107, 108). Equations 57 to 62 represent the analytical tension and moment calculations. Material models were adopted representing a low-strength steel and high-strength aluminum (Eqs 26, 27). Numerical integrations were carried out with three common choices of integration rules: trapezoidal (Ref 114), Simpson (Ref 115), or Gauss (Ref 116). Figure 18 presents the fractional moment error for the low-strength steel bent to $R/t = 5$ using a trapezoidal integration rule with 51 integration points through the thickness (N_{IP}) for various normalized sheet tension forces. (The normalized sheet tension force is defined by dividing the applied tension force by the force to yield the sheet, which is equal to the yield stress times width times thickness of the sheet.) The range of sheet tensions considered is from zero (pure bending case) to \bar{T}_{max} , where \bar{T}_{max} is the normalized sheet

tension force where the entire thickness of the sheet is plastically deforming; that is, the elastic core has moved to the edge of the sheet. For the low-strength steel at $R/t = 5$, \bar{T}_{max} is 2.06.

Two conclusions can be drawn from the set of computations shown in Fig. 18. First, the errors fall into a range depending on the exact choice of parameters. For some particular cases, the error may be zero, while at nearby adjacent states the error may be maximum. (For Fig. 18, this effect can be observed by small changes of the normalized tension force.) The behavior is oscillatory (as most easily seen in Fig. 18 at smaller tension forces), depending on where the integration points fall relative to the actual through-thickness stress distribution. The smooth lines drawn on Fig. 18 represent the assured error limit, that is, the limit of error in the vicinity of a

given set of conditions. For any set of conditions and numerical integration choices, the numerical integration error will always be less than or equal to this assured error limit, but the actual error in the nearby vicinity of those conditions may be anywhere from zero to this value. In this manner, the bounding error limit can be defined.

The second conclusion illustrated by Fig. 18 is that the assured fractional moment error (or, more succinctly, limiting error) increases for increasing sheet tension. This can be understood in terms of the decreasing moment with increasing sheet tension. Thus, a given absolute error in reproducing the analytical stress distribution by numerical integration technique represents a larger fractional error of moment (or springback). While assured fractional moment error is increased for larger sheet tensions, note that the

oscillatory behavior still exists, so it is possible in the vicinity of any sheet tension to obtain a particular result with nearly zero error. Such an isolated result is fortuitous and should not be relied on to estimate future performance.

A comparison of the three tested integration methods (Fig. 19) shows that no single integration method works best throughout the range of parameters. In view of the oscillatory nature of the error, for any given set of conditions, any one of these may outperform the other two. In Fig. 19, the unsigned assured error limit is presented. This error limit is smaller at low back forces for trapezoidal integration, while Gauss integration is better at higher normalized tension forces. This may be simply understood by noting that the stress distribution is smoothest in this region, most like a polynomial, and thus

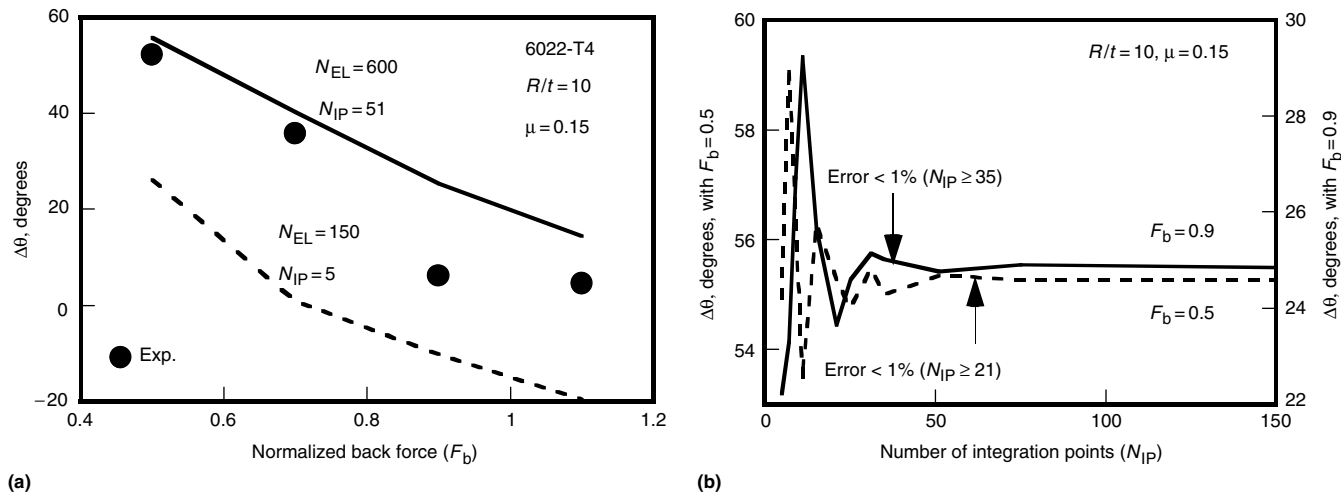


Fig. 17 Sensitivity of simulated draw-bend springback to mesh size (N_{EL}) and number of through-thickness integration points (N_{IP}). (a) Nonphysical springback predictions obtained using typical sheet-forming simulation parameters. (b) Accuracy of selected springback solutions depending on the number of through-thickness integration points. $\Delta\theta$, springback angle; R/t , ratio of bending radius to thickness; μ , friction coefficient

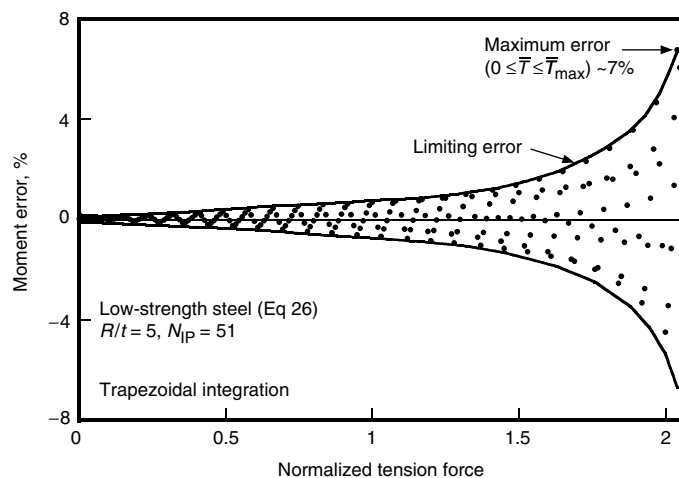


Fig. 18 Fractional error of computed moment (or springback) using trapezoidal integration and 51 integration points (N_{IP}) through the thickness. The limiting error (i.e., the assured maximum error in the vicinity of a set of conditions) is shown as smooth curves, and the maximum error occurs for a normalized tension force of 2.06 (\bar{T}_{max}). R/t , ratio of bending radius to thickness

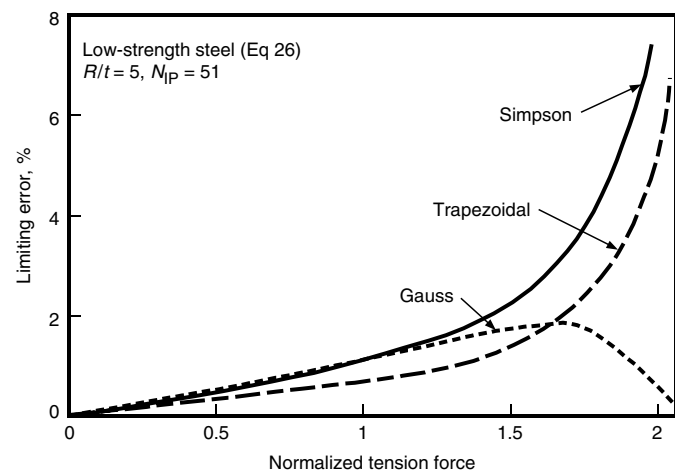


Fig. 19 Comparison of the variation of limiting error (unsigned) with normalized tension for three common integration schemes using 51 integration points (N_{IP}) through the thickness. R/t , ratio of bending radius to thickness

16 / Process Design for Sheet Forming

is reproduced better by Gauss integration in general. Because the largest possible fractional errors occur at larger tension forces, the Gauss integration scheme is a good choice (but by no means the best for all cases).

The role of R/t in affecting integration error is illustrated in Fig. 20. A maximum error is defined, as shown in Fig. 18 and as plotted in Fig. 20. That is, this quantity represents the assured fractional error limit for a range of normalized tension forces between 0 (pure bending) and \bar{T}_{\max} (where the entire thickness yields plastically in tension). This maximum error is of interest because for most forming operations, the value of the tension force is unknown except after the forming simulation is completed. Furthermore, it varies with time and location in the workpiece, as does R/t . Therefore, the maximum error must be considered as the numerical tolerance when performing a forming/springback simulation without *a priori* knowledge of the sheet tension. The maximum error is highest for small R/t values and lowest for larger R/t . Note the different scales on Fig. 20(a) and (b), illustrating the larger fractional errors for the low-strength steel.

A summary of many results such as those in Fig. 18 to 20 is presented in Fig. 21 and Table 5. Both may be used to determine the number of integration points needed to assure a limiting fractional error based only on numerical integration errors. (Of course, other sources of error, for example, incurred during the forming simulation or by other numerical aspects, can contribute to larger overall errors.) Note that Gauss integration is usually more efficient because, in the regime where the fractional springback errors are largest, it reproduces the analytical result best. The required number of integration points for a specified accuracy varies widely. For an assured 1% error tolerance, Gauss integration requires between 17 and 68 integration points through the thickness (depending on R/t and

material properties), while Simpson integration requires between 35 and 139 integration points through the thickness. For 10% tolerance, Gauss integration requires 5 to 16, depending on R/t and material properties, while Simpson requires 9 to 41.

Choice of Element, R/t , Anticlastic Curvature. Shell elements are preferred for springback simulation of sheet metal forming, because they can capture the bending behavior accurately while being computationally efficient as compared with solid elements, as long as the material thickness is small relative to the radius of bending. Membrane elements exclude bending effects and thus miss the major part of springback, while solid elements are very time-consuming for use with sheets because numerous layers must be used through the thickness (for the same reasons that many integration points are required for shells).

Draw-bend tests and simulations for drawing-quality special killed steel (Fig. 22a) showed that shell elements are accurate for R/t ratios as small as approximately 5 or 6, while solid elements are needed for smaller values, at much increased cost. Solid elements capture the through-thickness stresses that become significant for small R/t , but the typical brick elements with linear shape functions are very stiff in bending and provide poor results (Fig. 22b). For this reason, higher-order solid elements are preferred. For larger R/t ratios, shell elements normally provide better accuracy at much lower computation time.

One surprising result from the draw-bend simulations is that 3-D elements are required for the nominally 2-D problem (Fig. 22b). The answer lies in anticlastic curvature, discussed more fully in the section “Approximations in Classical Bending Theory” in this article. This is the secondary curvature that develops orthogonal to bending because of differential lateral contraction at the inner and outer

surfaces. As shown in Fig. 23, 3-D shell elements and 20-node quadratic solid elements capture the anticlastic curvature well, whereas 2-D elements and linear solid elements do not. Poor treatment of anticlastic curvature is the principal source of error in springback prediction for the draw-bend tests with back forces near the yield force. For arbitrary 3-D parts, the analog of anticlastic curvature causes distortion or wrinkling out of the plane of bending, as can be seen in the dimpling of the S-rail (Fig. 1a).

Unloading Scheme. Another surprising result from the draw-bend simulations is the importance, under some conditions, of plastic deformation during unloading. A comparison of 2-D simulation results is shown in Fig. 24, where the unloading was carried out purely elastically and elastic-plastically. Significant differences of the springback angle and residual stress are evident. However, it should be noted that in spite of the small plastic contribution to unloading behavior under some circumstances, the choice of path taken during unloading seems to have no significant effect on the final configuration (Ref 39). That is, the various unloading schemes and sequences for removing the tool constraints seem to give nearly identical results. It should also be noted that for many springback problems, particularly those with fairly small tension forces relative to yielding, the unloading will be purely elastic.

Plastic Constitutive Equation. At least two aspects of the plasticity law are important for springback prediction: plastic anisotropy (yield stress and strain ratios) and strain hardening. In particular, strain hardening must be suitable for a path reversal in draw-bend or channel-type forming, as is encountered when a material element undergoes sequential bending and unbending with superimposed tension (Ref 117). The yield surface anisotropy affects not only

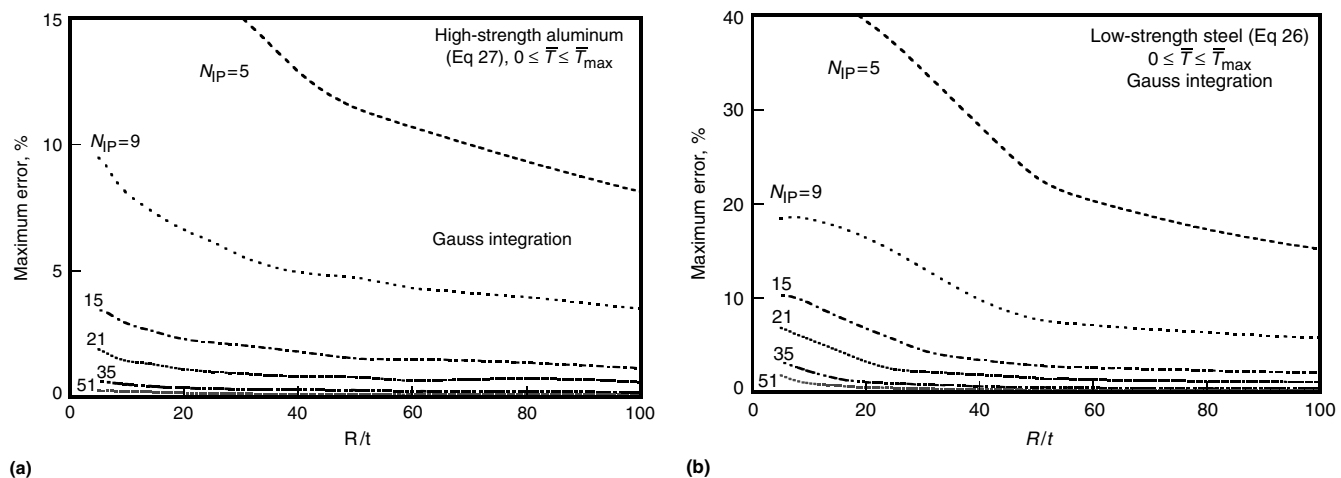


Fig. 20 The maximum error (that is, for sheet tensions from 0 to \bar{T}_{\max}) as a function of the ratio of bending radius to thickness (R/t) for various numbers of integration points (N_{ip}). (a) For material properties corresponding to a typical high-strength aluminum (Eq 27, $E = 70$ GPa, where E is Young's modulus). (b) For properties corresponding to typical low-strength steel (Eq 26, $E = 210$ GPa)

Springback / 17

the loaded bending moment but also the anticlastic curvature via the lateral strain ratios (related to the plastic anisotropy parameter, r , in various directions).

Table 6 compares the standard errors of fit for the simulated draw-bend springback angles for 6022-T4 aluminum alloy with $R/t = 10$ and normalized back forces ranging from 0.5 to 1.05.

Table 5 Number of through-thickness integration points (N_{IP}) required for a specified springback accuracy. Numbers without parentheses refer to Gauss integration; numbers in parentheses refer to Simpson integration

Maximum error	1%	5%	10%	50%
Low-strength steel ($0 \leq \bar{T} \leq \bar{T}_{max}$)				
$R/t = 5$	68 (139)	26 (69)	16 (41)	4 (9)
$R/t = 20$	38 (91)	18 (37)	13 (29)	4 (9)
$R/t = 100$	22 (57)	10 (23)	6 (15)	3 (7)
High-strength aluminum ($0 \leq \bar{T} \leq \bar{T}_{max}$)				
$R/t = 5$	30 (79)	13 (33)	9 (21)	4 (7)
$R/t = 20$	22 (55)	11 (25)	7 (15)	4 (7)
$R/t = 100$	17 (35)	8 (15)	5 (9)	3 (5)

\bar{T} , normalized sheet tension; R/t , ratio of bending radius to sheet thickness

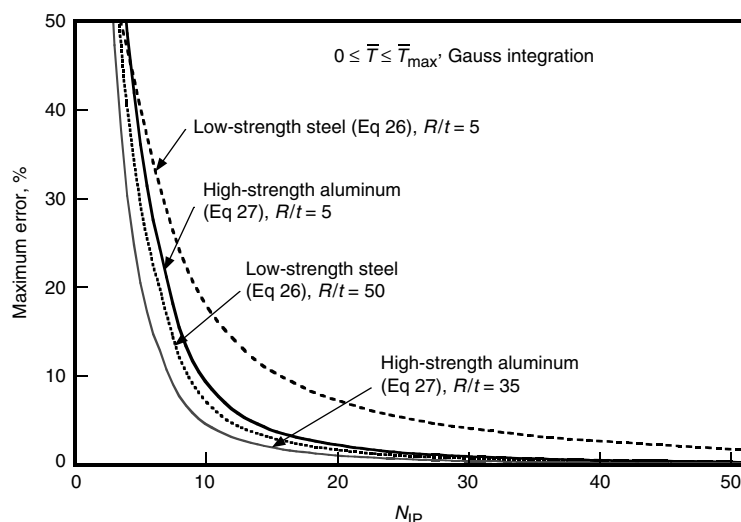


Fig. 21 Summary of the relationship between the maximum fractional error (for normalized sheet tension between 0 and \bar{T}_{max}) in moment (or springback) as a function of the number of integration points (N_{IP}) used with Gauss quadrature for several typical process and material parameters. R/t , ratio of bending radius to sheet thickness

The results illustrate that choosing an anisotropic yield function gives no guarantee of improved results. The Hill 48 quadratic yield function (Ref 23) gives significantly poorer fit than the von Mises isotropic yield function. The reason for this result is shown in Fig. 25, where the variation of yield stress and strain ratio with direction is poorly matched by the Hill 48 yield function and well represented by the Barlat YLD 96 (Ref 118) yield function. These results are presented and discussed in more detail in the literature (Ref 119), including excellent final prediction of anticlastic curvature. There are likely compensating effects of the yield stress variance and strain-ratio variance for the von Mises simulations that are not easily deconvoluted in predicting the final springback angle.

For all choices of yield function, taking into account the Bauschinger effect improves the prediction, as would be expected based on the reverse straining that takes place for most material elements throughout the draw-bend process (Ref 119).

Summary. The relative errors induced by the various factors discussed previously are illustrated in Fig. 26. Using normal forming simulation parameters (mesh size, integration points) and standard plastic laws (von Mises, isotropic hardening) for 2-D springback simulation leads to very poor results, including springback of the wrong sign (Fig. 17a, for example). The overall standard error of fit to the measured values is 26° . The 2-D simulations using adequately selected numerical parameters reduce the error to 19° (plane strain) and 11° (plane stress). Use of 3-D shell elements for simulation (i.e., taking anticlastic curvature into account) reduces the error to 5.7° . Incorporation of the proper yield function form, Barlat YLD 96 (Ref 118), and a treatment of the Bauschinger effect (Geng-Wagoner hardening, Ref 119) reduce the final error to 1.2° , approximately the same magnitude as the experimental scatter of the measurements.

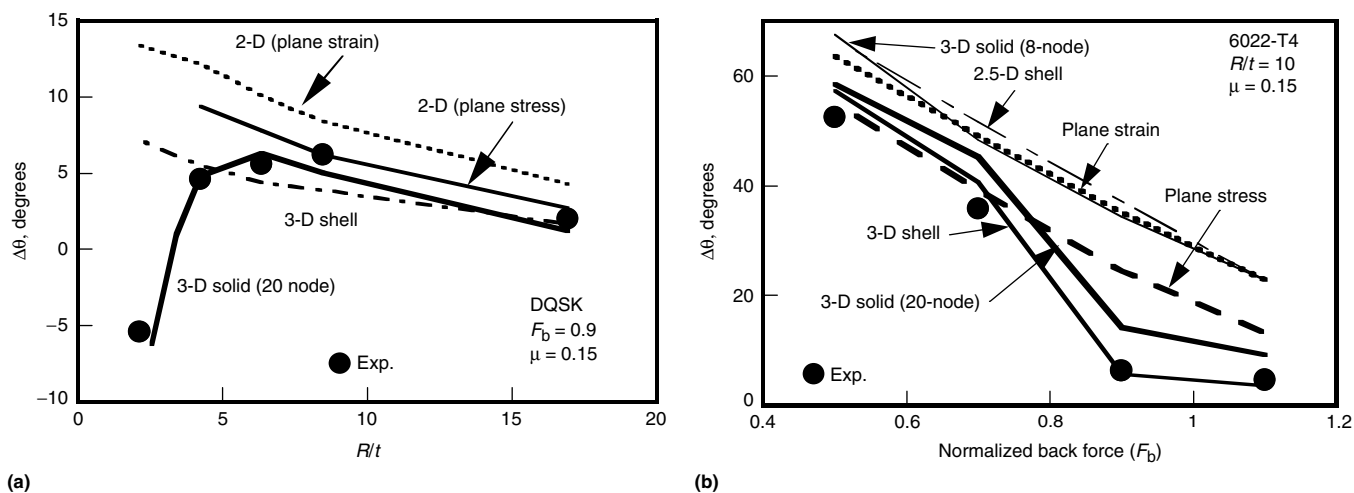


Fig. 22 The role of finite element type on draw-bend springback prediction. (a) Results for various R/t (bend radius/sheet thickness). (b) Results for various F_b (normalized back force). $\Delta\theta$, springback angle; DQSK, drawing quality special killed; μ , friction coefficient

18 / Process Design for Sheet Forming

Therefore, while it is essential to perform springback simulations carefully and to properly take into account the material behavior, it is possible to predict springback accurately for general cases. The biggest challenge for large-scale industrial applications lies with the convergence of implicit solutions during forming and the computational intensity of such simulations.

Springback Control and Compensation

The prediction of springback has been discussed in some detail at various levels of complexity in the foregoing sections. However, practical mitigation of springback in industry relies on two principal strategies: control (reduction) of springback via forming operation changes, and compensation for springback via changes of die shape. These two approaches

are discussed briefly, with references to original works provided.

Control of Springback. As illustrated in Fig. 10, application of sheet tension, particularly near the tension to yield of the sheet, drastically reduces springback by reducing the stress gradient through the thickness and hence the bending moment. Most industrial schemes for reducing springback rely on this principle. However, increasing sheet tension moves a forming operation closer to failure by splitting (Ref 47), such that many optimized forming operations walk a fine line between splitting and excessive springback.

Most springback control methods focus on increasing the sheet tension while mitigating the negative effect on formability. The tension can be applied during the drawing part of the forming operation or subsequently (Ref 48, 71). By the use of a variable blank-holder force throughout the punch stroke, the sheet tension can be varied arbitrarily (Ref 120–122). Alternatively, special

reverse-bending tooling may be devised either for pure bending (Ref 123, 124) or in the context of a more general channel forming (Ref 73, 125).

More general empirical approaches based on observations of numerous forming operations (Ref 126–129) involve a range of options including altering R/t , die clearances, punch bottoming, coining, and off-axis/in-plane compression.

Compensation of Springback. Instead of trying to reduce springback, which invokes penalties in formability, an alternative approach is to design dies that produce the desired final part shape after springback. (Usually, the die face for a sheet-formed part is very close to the desired part shape; therefore, springback moves the final part configuration away from the desired one.)

If springback prediction is considered a forward analysis, then a backward analysis is needed to use such results to modify a die design in order to achieve a given final part shape. For simple bending operations involving constant radii of curvature, dies can be designed to account for springback using handbook tables or closed-form solutions, which can be inverted to specify tool radii for desired final-part radii. For new or unusual materials, varying radii of curvature (i.e., arbitrary curves), or arbitrary or

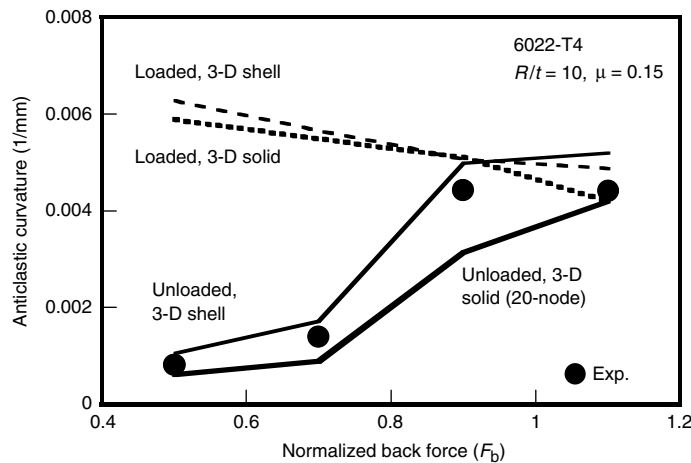


Fig. 23 Measured and simulated anticlastic curvature in the loaded and unloaded draw-bend specimens. R/t , ratio of bending radius to sheet thickness; μ , friction coefficient

Table 6 Standard errors of fit of simulated springback angle compared with measured ones for 6022-T4, $R/t=10$, $F_b=0.5$ to 1.05

Hardening law	Standard error of fit, degrees, for indicated yield function		
	von Mises	Hill 1948 (Ref 23)	Barlat YLD 96 (Ref 118)
Isotropic hardening	5.7	11.1	2.0
Geng-Wagoner hardening (Ref 95)	2.7	8.7	1.2

R/t, ratio of bending radius to sheet thickness; F_b , back force

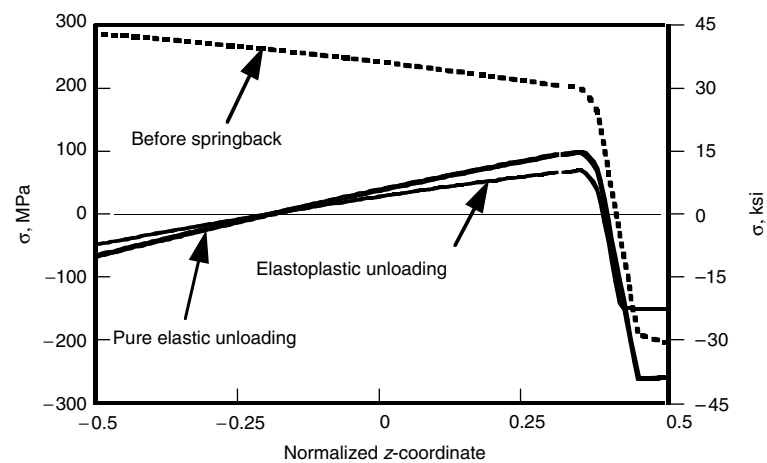
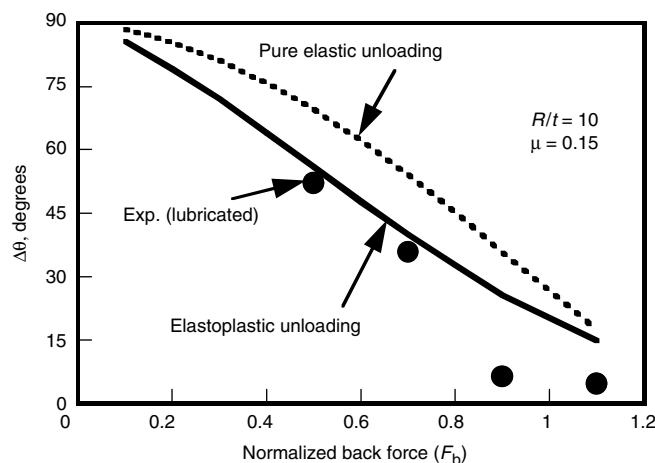


Fig. 24 Simulated role of plasticity in springback for a draw-bend test. (a) Difference of springback angle ($\Delta\theta$) for pure-elastic and elastoplastic springback simulations. (b) Differences in through-thickness stress distribution following pure-elastic and elastoplastic springback. R/t , ratio of bending radius to sheet thickness; μ , friction coefficient; σ , stress

Springback / 19

3-D shapes (with compound curvature), springback compensation has traditionally been carried out by simple trial and error or some variation thereof (Ref 130–132). Unfortunately, this procedure often produces unsatisfactory results and depends intimately on the skill and experience of the user. The process can take many months, thus extending critical tooling lead times. The trial-and-error method can be applied using FE forward analysis trials instead of experiments, but the backward design steps are equally inefficient and may take a similar amount of time.

Schemes for guiding the forward and backward analyses may be found in the literature based on various optimization strategies (Ref 89, 133, 134). These methods typically involve a gradient calculation and sensitivity analyses. Considerable complexity in formulation and implementation is involved, and usually special programming within special-purpose FE programs is required.

A promising approach integrating forward (FE) and backward analyses in an iterative scheme was reported by Karafilis and Boyce

(Ref 135–137). This method, denoted the springforward method, may in principle be used with any FE program. As discussed subsequently, however, its application suffers from lack of convergence (Ref 138, 139) unless the forming operation is symmetric or has very limited geometric change during springback (Ref 138).

Figure 27 outlines the steps of the springforward method. A flat sheet is first deformed into the target shape, and the external forces are recorded. At step 3, the target shape is elastically

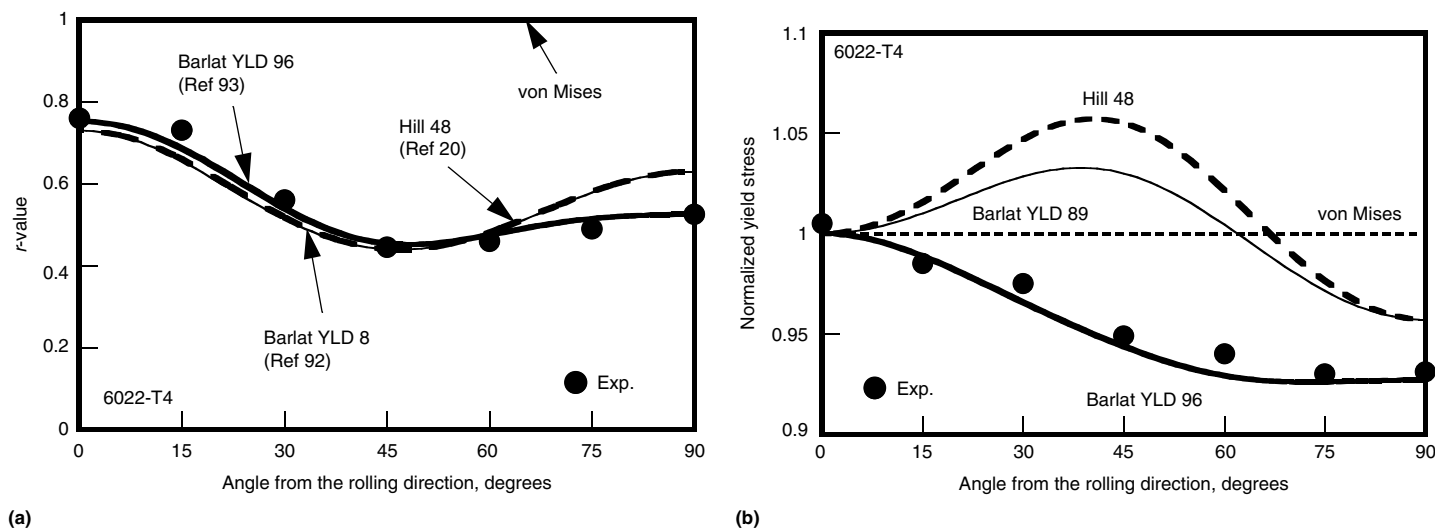


Fig. 25 Comparison of plasticity predictions for various in-plane sheet directions for several yield functions fit to a 6022-T4 aluminum alloy sheet. (a) Plastic anisotropy parameter (r -value). (b) Yield stresses normalized to yield stress in the rolling direction (0°)

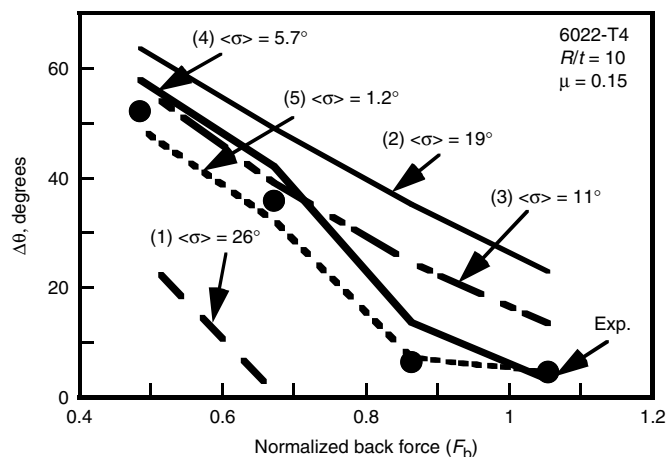


Fig. 26 The role of numerical procedures and constitutive modeling in springback accuracy as represented by standard error of fit, $\langle \sigma \rangle$, to measurement. Springback angles ($\Delta\theta$): (1) Plane stress, 5 integration points (N_{IP}), 600 elements along length (N_{EL}), von Mises yield, and isotropic hardening. (2) Plane strain, $N_{IP} = 51$, $N_{EL} = 600$, von Mises yield, and isotropic hardening. (3) Plane stress, $N_{IP} = 51$, $N_{EL} = 600$, von Mises yield, and isotropic hardening. (4) 3-D shell, $N_{IP} = 51$, $N_{EL} = 600$, von Mises yield, and isotropic hardening. (5) 3-D shell, $N_{IP} = 51$, $N_{EL} = 600$, Barlat 96 yield, and Geng-Wagoner anisotropic hardening. R/t , ratio of bending radius to sheet thickness; μ , friction coefficient

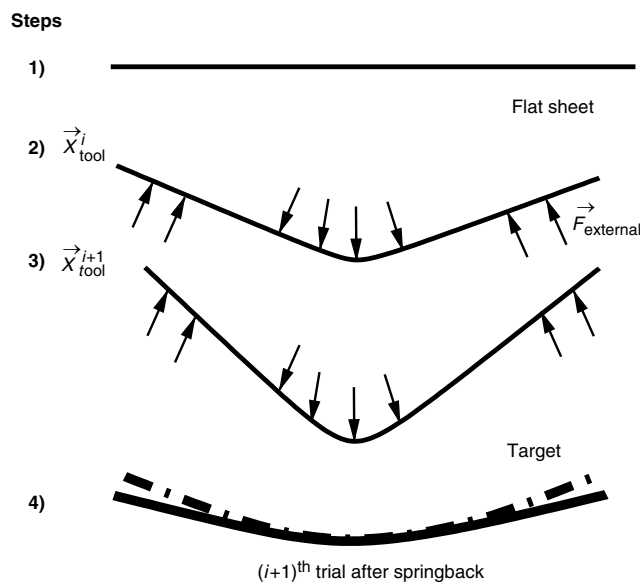


Fig. 27 Schematic representation of the steps undertaken in the springforward method of springback compensation. Step 1: flat sheet before deformation; Step 2: form to the tool shape and record external force field; Step 3: apply the recorded force field to the previous tooling shape and obtain the new tooling shape; Step 4: evaluate the $(i + 1)^{th}$ tooling shape by comparing the part shape, after forming and springback, with the target shape. \vec{X}_{tool}^i , forming tool position at i^{th} iteration; F , force. Source: Ref 135–137

20 / Process Design for Sheet Forming

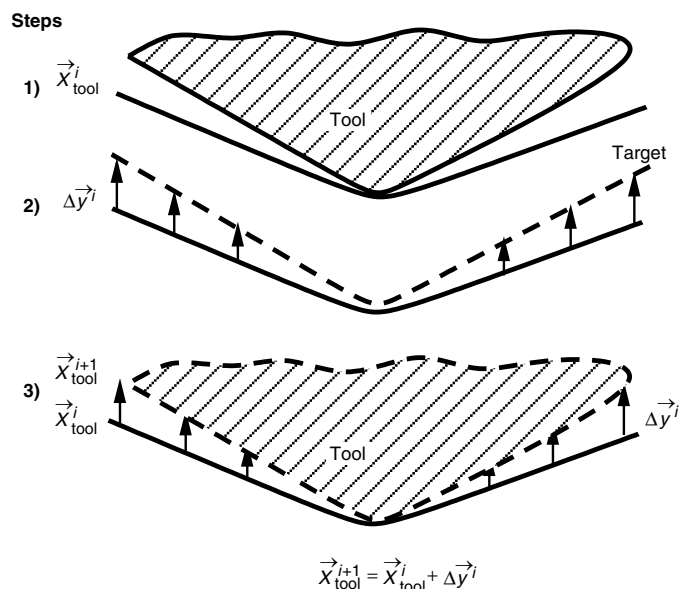


Fig. 28 Schematic representation of the steps undertaken in the Displacement Adjustment method of springback compensation. Step 1: form the part to the i^{th} tooling shape; Step 2: compare the part shape after springback with the target shape; Step 3: generate the $(i + 1)^{\text{th}}$ tooling shape by adding the displacement error field to the i^{th} tooling. X_{tool}^i , forming tool position at i^{th} iteration; Δy^i , the i^{th} displacement correction. Source: Ref 138

loaded by the recorded external forces, and the next trial die shape is obtained (the same shape as the deformed blank at the end of this step). This is the springforward step. The accuracy of the trial die shape is next checked by doing a forming and springback simulation. If the resulting springback shape is not the same as the target, another cycle will be carried out from step 1. Now, a flat sheet is deformed to the trial die shape just obtained, instead of being deformed to the target shape as in the first cycle. External forces are recorded and applied to the target shape. A new trial die shape will be obtained. The new trial die shape will be checked again at step 4, and iterations will continue until the target part shape is attained within a specified tolerance. Variations of this approach have been presented making use of internal forces instead of contact forces (Ref 137).

An alternate iterative design method that avoids many of the limitations of springforward while maintaining its generality and ease of implementation may be designated the displacement adjustment method (Ref 138). Instead of a springforward step using simulated contact forces, the simulated forming and springback displacements are used to predict the next die design iteration. A similar approach has been used in one-step simulation versions (Ref 140) and via experimental iteration (Ref 67, 141). The displacement adjustment method appears to offer several advantages over the springforward method, including excellent convergence rate, ease of implementation, and considerable generality. However, it has only been tested for rather simple 2-D, bending-dominated problems as of this writing.

The displacement adjustment method is outlined in Fig. 28. First, a flat sheet of metal is deformed to a trial die shape (for the first cycle, the trial die shape is the target shape). After springback, the springback shape is compared with its target. The shape error is defined as Δy^i , which is the vector difference of coordinates of a FE node in the springback shape and in the target shape, at the i^{th} iteration. At step 3, the Δy^i is added to the current die shape nodal positions, obtaining a new tooling shape of X_{tool}^{i+1} . For the next cycle, a flat sheet is deformed to this new tooling shape. If the springback shape is not within a specified tolerance of the target (checked at step 2), another iteration will be conducted.

Comparison of springforward and displacement adjustment methods for a simple bending-dominated forming operation have been presented (Ref 138). For an arbitrary, nonsymmetric, nonconstant-radius part shape (Ref 138), both methods were applied, with iterative results shown in Fig. 29. The normalized error for the n^{th} iteration cycle in Fig. 29 is defined as:

$$\frac{\text{rms error}^{(n)}}{\text{rms error}^{(1)}} \quad (\text{Eq 63})$$

where:

$$\text{rms error} = \left[\frac{\sum \Delta y_k^2}{N} \right]^{1/2} \quad (\text{Eq 64})$$

where rms is root mean square, K is a counting variable that progresses from 1 to N , and N is the total number of nodes of displacement.

Analysis of simpler, symmetric operations showed that the obstacle to applying the

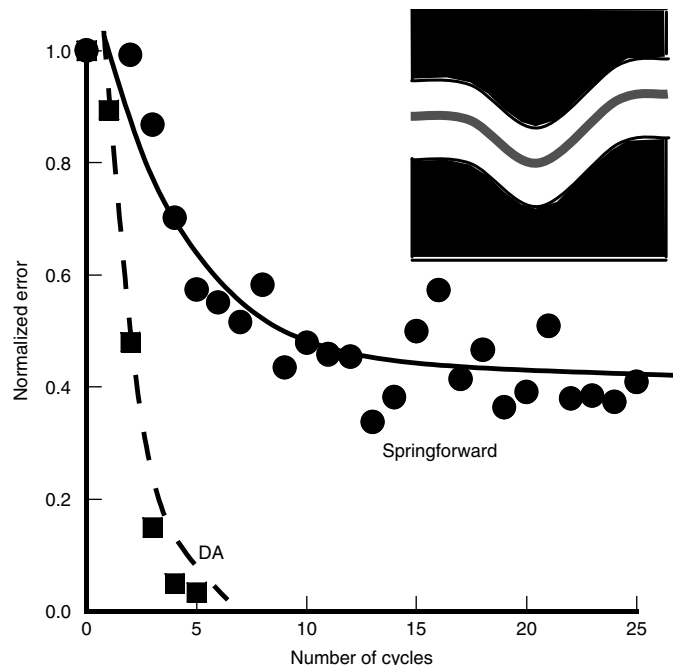


Fig. 29 Convergence and accuracy comparison of springforward and displacement adjustment (DA) springback compensation

springforward method lies with the unknown constraints that must be enforced during the springforward step to restrict rigid body motion. Unless such conditions are applied at exactly the right location, which usually is unknown for a general problem, the springforward forces distort the workpiece and lead to nonconvergence of the technique.

ACKNOWLEDGMENTS

The authors would like to thank the funding support of the National Science Foundation (DMR 0139045) and the Center for Advanced Materials and Manufacturing of Automotive Components at The Ohio State University. Computer simulations were conducted with the help of the Ohio Supercomputer Center (PAS080). Special thanks to Christine Putnam, who helped prepare the manuscript.

REFERENCES

1. J.K. Lee, G.L. Kinzel, and R.H. Wagoner, Ed., *Proceedings of NUMISHEET '96*, The Ohio State University (Columbus, OH), 1996
2. R. Böklen, *Z. Metallkd.*, Vol 44, 1953, p 382-386
3. C.A. Queener and R.J. DeAngelis, *Trans. ASME*, Vol 61, 1968, p 757-768
4. Z. Marciniak and J.L. Duncan, *Mechanics of Sheet Metal Forming*, 1st ed., Edward Arnold, London, England, 1992

5. Z. Marciniak, J.L. Duncan, and S.J. Hu, *Mechanics of Sheet Metal Forming*, 2nd ed., Butterworth-Heinemann, 2002
6. W.F. Hosford and R.M. Caddell, *Metal Forming: Mechanics and Metallurgy*, 2nd ed., Prentice Hall, 1993
7. K.C. Chan and S.H. Wang, *J. Mater. Process. Technol.*, Vol 91, 1999, p 111–115
8. W. Schroeder, *J. Appl. Mech. (Trans. ASME)*, Vol 65, 1943, p 817–827
9. T.X. Yu and L.C. Zhang, *Plastic Bending, Theory and Applications*, World Scientific, 1996
10. W.C. Young, Table I, Case 20, *Roark's Formulas for Stress and Strain*, 6th ed., McGraw-Hill, 1989, p 68
11. B.W. Shaffer and E.E. Ungar, *J. Appl. Mech. (Trans. ASME)*, Vol 82, 1960, p 34–40
12. S.H. Crandall and N.C. Dahl, *Introduction to the Mechanics of Solids*, McGraw-Hill, 1961, p 327–336
13. J.D. Lubahn and G. Sachs, *Trans. ASME*, Vol 72, 1950, p 201–208
14. F.J. Gardiner, *J. Appl. Mech. (Trans. ASME)*, Vol 79, 1957, p 1–9
15. J.M. Alexander, An Analysis of the Plastic Bending of Wide Plate, and the Effect of Stretching on Transverse Residual Stress, *Proc. Inst. Mech. Eng.*, Vol 173 (No. 1), 1959, p 73–96
16. G. Sachs, *Principles and Methods of Sheet-Metal Fabricating*, Reinhold, 1951
17. J.H. Hollomon, *A.I.M.E. Trans.*, Vol 162, 1945, p 268
18. D.M. Woo and J. Marshall, *The Engineer*, Vol 208, 1959, p 135–136
19. Z.T. Zhang and S.J. Hu, "Mathematical Bending in Plane Strain Bending," Paper 970439, Society of Automotive Engineers, 1997
20. User Manual, ABAQUS Standard, Version 6.2, ABAQUS, Inc., Pawtucket, RI, 2002
21. A.K. Sachdev and R.H. Wagoner, Uniaxial Strain Hardening at Large Strain in Several Sheet Steels, *J. Appl. Metalwork.*, Vol 3 (No. 1), 1983, p 32
22. *Properties of Some Metals and Alloys*, 3rd ed., The International Nickel Company, Inc., 1968, p 14
23. R. Hill, Theory of Yielding and Plastic Flow of Anisotropic Metals, *Proc. R. Soc. (London)*, 1948, p 193–281
24. Z.T. Zhang and D. Lee, "Effect of Process Variables and Material Properties on the Springback Behavior of 2-D Draw Bending Parts," Paper 950692, Society of Automotive Engineers, 1995
25. E.A. Popov, *Russ. Eng. J.*, Vol 43 (No. 10), 1963, p 39–40
26. H. Lamb, *Philos. Mag.*, Vol 31, 1891, p 182–195
27. H.D. Conway and W.E. Nickols, *Exp. Mech.*, Vol 5, 1965, p 115–119
28. D.G. Ashwell, *J. R. Aero. Soc.*, Vol 54, 1950, p 708–715
29. D. Horrocks and W. Johnson, *Int. J. Mech. Sci.*, Vol 9, 1967, p 835–861
30. G.F.C. Searle, *Experimental Elasticity: A Manual for the Laboratory*, Cambridge University Press, Cambridge, England, 1908
31. J. Case, *Strength of Materials*, 3rd ed., Arnold, 1938, p 645–654
32. C.T. Wang, G. Kinzel, and T. Altan, *J. Mater. Process. Technol.*, Vol 39, 1993, p 279–304
33. R. Hill, *The Mathematical Theory of Plasticity*, Oxford University Press, London, England, 1950
34. R.H. Wagoner, *Metall. Trans. A*, Vol 11, 1980, p 165–175
35. R.H. Wagoner, *Metall. Trans. A*, Vol 12, 1981, p 2142–2145
36. T.X. Yu and W. Johnson, *J. Mech. Work. Technol.*, Vol 6, 1982, p 5–21
37. K.P. Li and R.H. Wagoner, Simulation of Springback, *Simulation of Materials Processing, Proceedings of NUMIFORM '98* (Enschede, Netherlands), 1998, p 21–31
38. K.P. Li, L.M. Geng, and R.H. Wagoner, Simulation of Springback: Choice of Element, *Advanced Technology of Plasticity, Proceedings of the Sixth ICTP* (Nuremberg, Germany), Vol III, 1999a, p 2091–2098
39. K.P. Li, L.M. Geng, and R.H. Wagoner, Simulation of Springback with the Draw/Bend Test, *Proceedings of IPMM '99* (Vancouver, B.C., Canada), 1999b, p 1
40. K.P. Li, W.P. Carden, and R.H. Wagoner, *Int. J. Mech. Sci.*, Vol 44, 2002, p 103–122
41. R.H. Wagoner, W.D. Carden, W.P. Carden, and D.K. Matlock, Springback after Drawing and Bending of Metal Sheets, *Proceedings, IPMM '97—Intelligent Processing and Manufacturing of Materials*, University of Wollongong, Vol 1, 1997, p 1–10
42. J.F. Wang, R.H. Wagoner, and D.K. Matlock, Creep following Springback, *Proceedings, Tenth Conference of Plasticity* (Quebec City, Canada), 2003, p 211–213
43. R.M. Cleveland and A.K. Ghosh, *Int. J. Plast.*, Vol 28, 2002, p 769–785
44. F. Morestin and M. Boivin, *Nucl. Eng. Des.*, Vol 162, 1996, p 107–116
45. H.W. Swift, *Engineering*, Oct 1948, p 333–359
46. M.L. Wenner, Report MA-233, General Motors Research Laboratories, May 1982
47. M.L. Wenner, *J. Appl. Metalwork.*, Vol 2 (No. 4), 1983, p 277–287
48. M.K. Mickalich and M.L. Wenner, Report GMR-6108, General Motors Research Laboratories, Feb 1988
49. J.L. Duncan and J.E. Bird, Approximate calculations for Draw Die Forming and Their Application to Aluminium Alloy Sheet, *Proceedings of the Tenth Biennial Cong. IDDRG*, (Warwick, England), Vol 1, The International Deep Drawing Research Group, April 1978, p 45–52
50. J.L. Duncan and J.E. Bird, *Sheet Met. Ind.*, Vol 55 (No. 9), Sept 1978, p 1015–1023
51. T. Kuwabara, S. Takahashi, K. Akiyama, and Y. Miyashita, "2-D Springback Analysis for Stretch-Bending Processes Based on Total Strain Theory," Paper 950691, Society of Automotive Engineers, 1995, p 1–10
52. T. Kuwabara, S. Takahashi, and K. Ito, Springback Analysis of Sheet Metal Subjected to Bending-Unbending under Tension I, *Advanced Technology of Plasticity, Proceedings of the Fifth ICTP* (Columbus, OH), Vol 2, 1996, p 743–746
53. S. Takahashi, T. Kuwabara, and K. Ito, Springback Analysis of Sheet Metal Subjected to Bending-Unbending under Tension II, *Advanced Technology of Plasticity, Proceedings of the Fifth ICTP* (Columbus, OH), Vol 2, 1996, p 747–750
54. T. Kuwabara, N. Sekiand, and S. Takahashi, A Rigorous Numerical Analysis of Residual Curvature of Sheet Metals Subjected to Bending-Unbending under Tension, *Advanced Technology of Plasticity, Proceedings of the Sixth ICTP* (Nuremberg, Germany), Vol 2, 1999, p 1071–1076
55. W.Y.D. Yuen, *J. Mater. Process. Technol.*, Vol 22, 1990, p 1–20
56. R. Hino, Y. Goto, and M. Shiraishi, Springback of Sheet Metal Laminates Subjected to Stretch Bending and the Subsequent Unbending, *Advanced Technology of Plasticity, Proceedings of the Sixth ICTP* (Nuremberg, Germany), Vol 2, Sept 19–24, 1999, p 1077–1082
57. A.A. El-Domiatiy, M.A.N. Shabara, and M.D. Al-Ansary, *Int. J. Mach. Tools Manuf.*, Vol 36 (No. 5), 1996, p 635–650
58. W. Johnson and T.X. Yu, *Int. J. Mech. Sci.*, Vol 23, 1981, p 687–696
59. C. Sudo, M. Kojima, and T. Matsuoka, Some Investigations on Elastic Recovery of Press Formed Parts of High Strength Steel Sheets, *Proceedings of the Eighth Biennial Congress of IDDRG* (Gothenburg, Sweden), Vol 2, The International Deep Drawing Research Group, Sept 1974, p 192–202
60. M.L. Chakhari and J.N. Jalinier, Springback of Complex Parts, *Proceedings of the 13th Biennial Congress of IDDRG* (Melbourne, Australia), The International Deep Drawing Research Group, Feb 1984, p 148–159
61. L.C. Zhang and Z. Lin, *J. Mater. Process. Technol.*, Vol 63, 1997, p 49–54
62. A. Focellese, L. Fratini, F. Gabrielli, and F. Micari, *J. Mater. Process. Technol.*, Vol 80–81, 1998, p 108–112
63. H. Ogawa and A. Makinouchi, Small Radius Bending of Sheet Metal by

22 / Process Design for Sheet Forming

- Indentation with V-Shape Punch, *Advanced Technology of Plasticity, Proceedings of the Sixth ICTP* (Nuremberg, Germany), Vol 2, Sept 19–24, 1999, p 1059–1064
64. B.S. Levy, *J. Appl. Metalwork.*, Vol 3 (No. 2), 1984, p 135–141
 65. S.S. Han and K.C. Park, An Investigation of the Factors Influencing Springback by Empirical and Simulative Techniques, *Proceedings of NUMISHEET '99* (Besancon, France), 1999, p 53–57
 66. L.R. Sanchez, D. Robertson, and J.C. Gerdeen, "Springback of Sheet Metal Bent to Small Radius/Thickness Ratios," Paper 960595, Society of Automotive Engineers, 1996, p 650–656
 67. C. Wang, An Industrial Outlook for Springback Predictability, Measurement Reliability, and Compensation Technology, *Proceedings of NUMISHEET 2002* (Jeju Island, Korea), 2002, p 597–604
 68. R.G. Davies, *J. Appl. Metalwork.*, Vol 1, (No. 4), 1981, p 45–52
 69. F. Pourboghrat and E. Chu, *Int. J. Mech. Sci.*, Vol 36 (No. 3), 1995, p 327–341
 70. F. Pourboghrat and E. Chu, *J. Mater. Process. Technol.*, Vol 50, 1995, p 361–374
 71. R.G. Davies, *J. Appl. Metalwork.*, Vol 3 (No. 2), 1984, p 120–126
 72. N.E. Thompson and C.H. Ellen, *J. Appl. Metalwork.*, Vol 4 (No. 1), 1985, p 39–42
 73. Y.C. Liu, *J. Eng. Mater. Technol. (Trans. ASME)*, Vol 110, 1988, p 389–394
 74. W.D. Carden, L.M. Geng, D.K. Matlock, and R.H. Wagoner, *Int. J. Mech. Sci.*, Vol 44, 2002, p 79–101
 75. A. Makinouchi, E. Nakamachi, E. Onate, and R.H. Wagoner, Ed., *Proceedings of NUMISHEET '93* (Isehara, Japan), The Institute of Physical and Chemical Research, 1993
 76. S.F. Shen and P.R. Dawson, Ed., *Simulation of Materials Processing: Theory, Methods and Applications*, A.A. Balkema, Rotterdam, Holland, 1995
 77. J.C. Gelin and P. Picart, Ed., *Proceedings of NUMISHEET '99* (Besancon, France), Burs Publications, 1999
 78. D.-Y. Yang, S.I. Oh, H. Huh, and Y.H. Kim, Ed., *NUMISHEET 2002—Proc. Fifth Int. Conf. Workshop Num. Simul. 3D Sheet Forming Processes* (Jeju, Korea), Vol 1, 2002
 79. K. Mattiasson, A. Strange, P. Thilderkvist, and A. Samuelsson, Simulation of Springback in Sheet Metal Forming, *Proceedings of the Fifth International Conference on Numerical Methods in Industrial Forming Process* (New York), 1995, p 115–124
 80. S.W. Lee and D.Y. Yang, *J. Mater. Process. Technol.*, Vol 80–81, 1998, p 60–67
 81. S.C. Tang, Analysis of Springback in Sheet Forming Operation, *Advanced Technology of Plasticity, Proceedings, Second ICTP* (Stuttgart, Germany), Vol 1, 1987, p 193–197
 82. N. He and R.H. Wagoner, Springback Simulation in Sheet Metal Forming, *Proceedings of NUMISHEET '96* (Columbus, OH), 1996, p 308–315
 83. N. Narasimhan and M. Lovell, *Finite Elem. Anal. Des.*, Vol 33, 1999, p 29–42
 84. Y. Hu and C. Du, Quasi Static Finite Element Algorithms for Sheet Metal Stamping Springback Simulation, *Proceedings of NUMISHEET '99* (Besancon, France), 1999, p 71–76
 85. L.M. Geng and R.H. Wagoner, Springback Analysis with a Modified Hardening Model, Sheet Metal Forming, *Sing Tang 65th Anniversary Volume*, SP-1536, SAE Publication 2000-01-0768, Society of Automotive Engineers, 2000, p 21–32
 86. D.W. Park, J.J. Kang, J.P. Hong, and S.I. Oh, Springback Simulation by Combined Method of Explicit and Implicit FEM, *Proceedings of NUMISHEET '99* (Besancon, France), 1999, p 35–40
 87. F. Valente and D. Traversa, Springback Calculation of Sheet Metal Parts after Trimming and Flanging, *Proceedings of NUMISHEET '99* (Besancon, France), 1999, p 59–64
 88. N. Montmayeur and C. Staub, Springback Prediction with OPTRIS, *Proceedings of NUMISHEET '99* (Besancon, France), 1999, p 41–46
 89. G.Y. Li, M.J. Tan, and K.M. Liew, *Int. J. Solids Struct.*, Vol 36 (No. 30), Oct 1999, p 4653–4668
 90. U. Abdelsalam, A. Sikorski, and M. Karima, Application of One Step Springback for Product and Early Process Feasibility on Sheet Metal Stampings, *Proceedings of NUMISHEET '99* (Besancon, France), 1999, p 47–52
 91. R.H. Wagoner and J.-L. Chenot, *Metal Forming Analysis*, Cambridge University Press, Cambridge, U.K., 2001
 92. R.D. Cook, D.R. Malkus, M.E. Plesha, R.J. Witt, *Concepts and Applications of Finite Element Analysis*, 4th ed., Wiley, 2002
 93. J.N. Reddy, *Introduction to the Finite Element Method*, 2nd ed., McGraw-Hill, 1993
 94. O.C. Zienkiewicz and R.L. Taylor, *The Finite Element Method: Volume 1, The Basis*, 5th ed., Butterworth-Heinemann, Oxford, U.K., 2000
 95. O.C. Zienkiewicz and R.L. Taylor, *The Finite Element Method: Volume 2, Solid Mechanics*, 5th ed., Butterworth-Heinemann, Oxford, U.K., 2000
 96. T.J.R. Hughes, *The Finite Element Method: Linear Static and Dynamic Analysis*, Prentice-Hall, 1987
 97. K.-J. Bathe, *Finite Element Procedures*, Prentice-Hall, 1995
 98. http://www.abaqus.com/products/products_standard.html, ABAQUS, Inc., 2005
 99. <http://www.ansys.com/products/mechanical.asp>, ANSYS, Inc., 2005
 100. http://www.abaqus.com/products/products_explicit.html, ABAQUS, Inc., 2005
 101. <http://www.lstc.com>, Livermore Software Technology Corp., 2005
 102. J. Wang and R.H. Wagoner, A New Hexahedral Solid Element for 3D FEM Simulation of Sheet Metal Forming, *Proc. of NUMIFORM 2004, Materials Processing and Design* (Columbus, OH), S. Ghosh, J.M. Casto, and J.K. Lee, Ed., June 2004, p 2181–2186
 103. J. Wang and R.H. Wagoner, A Practical Large Strain Solid Finite Element for Sheet Forming, *Int. J. Numer. Methods Eng.*, in press
 104. T. Shimizu, E. Massoni, N. Soyris, and J.-L. Chenot, A Modified 3-Dimensional Finite Element Model for Deep-Drawing Analysis, *Advances in Finite Deformation Problems in Material Processing and Structure*, N. Chandra et al., Ed., AMD Vol 125, ASME, 1991, p 113–118
 105. M. Kawka and A. Makinouchi, Finite Element Simulation of Sheet Metal Forming Processes by Simultaneous Use of Membrane, Shell and Solid Elements, *Numerical Methods in Industrial Forming Processes*, J.-L. Chenot et al., Ed., Balkema, Rotterdam, 1992, p 491–496
 106. K.P. Li and R.H. Wagoner, Simulation of Deep Drawing with Various Elements, *Proceedings of NUMISHEET '99* (Besancon, France), 1999, p 151–156
 107. A. Andersson and S. Holmberg, Simulation and Verification of Different Parameters Effect on Springback Results, *Proceedings of NUMISHEET 2002* (Jeju Island, Korea), 2002, p 201–206
 108. V.T. Nguyen, Z. Chen, et al., Prediction of Spring-Back in Anisotropic Sheet Metals, *Proc. Inst. of Mech. Eng. C, J. Mech. Eng. Sci.*, Vol 218 (No. 6), 2004, p 651–661
 109. W.L. Xu, C.H. Ma, et al., Sensitive Factors in Springback Simulation for Sheet Metal Forming, *J. Mater. Process. Technol.*, Vol 151 (No. 1–3), 2004, p 217–222
 110. N. Yamamura, T. Kuwabara, et al., Springback Simulations for Stretch-Bending and Draw-Bending Processes Using the Static Explicit FEM Code, with an Algorithm for Canceling Non-equilibrated Forces, *Proceedings of NUMISHEET 2002* (Jeju Island, Korea), 2002, p 25–30
 111. H. Yao, S.-D. Liu, et al., Techniques to Improve Springback Prediction Accuracy Using Dynamic Explicit FEA Codes, *SAE Trans. J. Mater. Manuf.*, Vol 111, 2002, p 100–106
 112. R.H. Wagoner and M. Li, Advances in Understanding Springback Simulations, *Proceedings of NUMISHEET 2005*, 2005
 113. R.H. Wagoner and M. Li, Sheet Simulation of Springback: Through-Thickness Integration, *Int. J. Numer. Methods Eng.*, submitted
 114. E.W. Weisstein, Trapezoidal Rule, *MathWorld—A Wolfram Web Resource*, <http://>

Springback / 23

- mathworld.wolfram.com/TrapezoidalRule.html, 2005
115. E.W. Weisstein, Simpson's Rule, *MathWorld—A Wolfram Web Resource*, <http://mathworld.wolfram.com/SimpsonsRule.html>, 2005
 116. E.W. Weisstein, Legendre-Gauss Quadrature, *MathWorld—A Wolfram Web Resource*, <http://mathworld.wolfram.com/Legendre-GaussQuadrature.html>, 2005
 117. S.C. Tang, Application of an Anisotropic Hardening Rule to Springback Prediction, *Advanced Technology of Plasticity, Proceedings, Fifth ICTP* (Columbus, OH), Vol 2, 1996, p 719–722
 118. F. Barlat, Y. Maeda, K. Chung, M. Yanagawa, J.C. Brem, Y. Hayashida, D.J. Legfe, S.J. Matsui, S.J. Murtha, S. Hattori, R.C. Becker, and S. Makosey, *J. Mech. Phys. Solids*, Vol 45 (No. 11/12), 1997, p 1727–1763
 119. L.M. Geng and R.H. Wagoner, *Int. J. Mech. Sci.*, Vol 44, 2002, p 123–148
 120. Y. Hishida and R.H. Wagoner, SAE paper 930285, *J. Mater. Manuf.*, Vol 102, 1993, p 409–415
 121. D. Schmoeckel and M. Beth, *Ann. CIRP*, Vol 42 (No. 1), 1993, p 339–342
 122. M. Sunseri, J. Cao, A.P. Karafillis, and M.C. Boyce, *Trans. ASME*, Vol 118, 1996, p 426–435
 123. C.C. Chu, *Int. J. Solids Struct.*, Vol 22 (No. 10), 1986, p 1071–1081
 124. Y. Nagai, *Jpn. Soc. Technol. Plast.*, Vol 28, 1987, p 143–149
 125. R.A. Ayres, *J. Appl. Metalwork.*, Vol 3 (No. 2), 1984, p 127–134
 126. Y. Hayashi, Analysis of Surface Defects and Side Wall Curl in Press Forming, *Proceedings of the 13th Biennial Congress of IDDRG* (Melbourne, Australia), The International Deep Drawing Research Group, Feb 1984, p 565–580
 127. Y. Tozawa, *J. Mater. Process. Technol.*, Vol 22, 1990, p 343–351
 128. Y. Umehara, *J. Mater. Process. Technol.*, Vol 22, 1990, p 239–256
 129. M. Ueda and K. Ueno, *J. Mech. Work. Technol.*, Vol 5, 1981, p 163–179
 130. R.D. Webb, "Spatial Frequency Based Closed-Loop Control of Sheet Metal Forming," Ph.D. thesis, Massachusetts Institute of Technology, 1987
 131. R.D. Webb and D.E. Hardt, *J. Eng. Ind. (Trans. ASME)*, Vol 113, 1991, p 44–52
 132. C. Hindman and K.B. Ousterhout, *J. Mater. Process. Technol.*, Vol 99, 2000, p 38–48
 133. O. Ghouati, D. Joannic, and J.C. Gelin, Optimisation of Process Parameters for the Control of Springback in Deep Drawing, *Proceedings of NUMIFORM '98* (Netherlands), 1998, p 819–824
 134. I. Chou and C. Hung, *Int. J. Mach. Tools Manuf.*, Vol 39, 1999, p 517–536
 135. A.P. Karafillis and M.C. Boyce, *Int. J. Mech. Sci.*, Vol 34 (No. 2), 1992, p 113–131
 136. A.P. Karafillis and M.C. Boyce, *J. Mater. Process. Technol.*, Vol 32, 1992, p 499–508
 137. A.P. Karafillis and M.C. Boyce, *Int. J. Mach. Tools Manuf.*, Vol 36 (No. 4), 1996, p 503–526
 138. W. Gan and R.H. Wagoner, Die Design Method for Sheet Springback, *Int. J. Mech. Sci.*, Vol 46 (No. 7), 2004, p 1097–1113
 139. R. Lingbeek, J. Huétink, S. Ohnimus, M. Petzoldt, and J. Weiher, The Development of a Finite Elements Based Springback Compensation Tool for Sheet Metal Products, *J. Manuf. Prod. Technol.*, in press
 140. F. Valente, X.P. Li, and A. Messina, in *Proceedings of Fourth COMPLAS* (Barcelona, Spain), Vol 2, 1997, p 1431–1488
 141. E. Chu, L. Zhang, S. Wang, X. Zhu, and B. Maker, Validation of Springback Predictability with Experimental Measurements and Die Compensation for Automotive Panels, *Proceedings of NUMISHEET 2002* (Jeju Island, Korea), 2002, p 313–318